

Authors response to Referee n° 1

We are thankful for the constructive and helpful comments that have helped us to improve our manuscript. We are aware that the manuscript holds a high amount of data which can be difficult to follow at some points and tried to keep it as concise as possible. We considered all comments carefully and modified and followed most of the suggestions.

Specific Comments from Referee n° 1

2) The introduction reads well. One question is whether you have a testable hypothesis. Are you trying to ask whether the corals are fueled by fluids versus scavenging from currents. How are you going to distinguish between mechanisms?

Response: the aim of the study is to address the linkage between CWCs and present day formation of MDACs in the Pompeia Province. For this purpose, we combined analyses of ROV images, geophysical data and sample materials. For instance, we analyzed $\delta^{13}\text{C}$ signatures of coral skeletons to evaluate whether these organisms were directly relying on CH_4 . We found that the coral skeletons exhibited significantly higher $\delta^{13}\text{C}$ values than the co-occurring AOM-derived carbonates, thus not supporting CH_4 as important carbon source. Rather, the corals were feeding on material suspended in currents.

3) In the methods please add section in which you describe the Experimental Design. How many samples were collected and from where? The descriptions of the laboratory methods are okay. However, I have no idea if you sampled thoroughly enough.

Response: we included more detailed information on our sample strategy and study design in the material and methods section.

4) In Table 2, will readers know what Identifier means? I realize that the numbers correspond to pictures in the figures. However, it is very confusing to have to put the figure next to the table to interpret the data in the table. There must be a better way to present the data.

Response: done. We replaced “Identifier” by “Identification number in Fig. 7”. In Addition, we added an additional column to the table in which we provide information on the analyzed material.

5) Rather than using code numbers for the sampling sites, it would help readers if you used descriptive names, such as ‘active seep’, etc.

Response: done. We have revised the use of code numbers throughout the manuscript.

6) Although amplicon sampling for microbial group is okay. Do you have evidence for microbial growth and activity? Perhaps in the discussion indicate which samples come from fresh material and are likely to have fresh DNA versus samples in which the DNA could be old and preserved. I realized this is inferred by looking at the pictures, but again this is a convoluted way to present a story.

Response: we have improved the information concerning the DNA material related to each sample in the manuscript, and we have specified the type of sample from which the DNA has been extracted (lines 155–158 in the revised manuscript). Furthermore, we added some extra information in Fig. 11 to clarify and

remain the type of sample. DNA analyses cannot conclude if DNA is “old” or “fresh”, but we can estimate (together with other analyses) if the sample used for this analysis is fresh or not. but we can infer this by assessing the relative age and preservation of the analyzed sample. For instance, a AOM-derived carbonate recovered from an active pockmark (sample D10-R7) exhibits more DNA of AOM-related microorganisms (ANME and SRB) than oxidized AOM-derived carbonates recovered from regions that are currently not affected by seepage (sample D10-R3).

7) I suppose the model is okay. However, again a better presentation of the data might lead readers to the conclusion rather than relying on the author’s story.

Response: done. We have modified the last paragraph of the section 4.3. for a better understanding of our model (lines 398–405 in the revised manuscript).

Technical Comments from Referee n° 1

1) Line 19: consider saying, ‘rate a seepage via focused, scattered, diffused, etc.’

Response: done. We revised the sentence to “the type of seepage such as focused, scattered, diffused or eruptive”.

2) Line 34: change ‘which’ to ‘that’.

Response: done.

3) Line 36: change to ‘typically, they thrive, etc.’

Response: done.

4) Line 45: change ‘ecological’ to ‘environmental’ and ‘are discussed to control’ to ‘influence’.

Response: done.

5) Line 51: delete ‘e.g.’.

Response: done.

6) Line 53: change ‘e.g.’ to ‘for example’.

Response: done.

7) Line 65: delete ‘i.e.’ and the parentheses. The text is not an example rather it is the description of ‘coral graveyards.’

Response: done.

Authors response to Referee n° 2

We are thankful for your constructive feedback and the helpful comments. We have considered and addressed your suggestions carefully, and almost all have been followed in the revised manuscript.

Detail Comments from Referee n° 2

1) Line 1. Title. The text after the hyphen: ‘living on the edge’ is unnecessary and adds nothing to the title. What edge? I suggest removing this.

Response: we would like to keep the text “living on the edge” to emphasize that hydrocarbon-rich seepage has both advantages and disadvantages for cold-water corals growth.

2) Lines 26-27. Abstract Delta C13 values of the coral skeletons (see below)

Response: see discussion on reviewer comment n° 19 below.

3) Line 31. Abstract. Suggest ‘seeping’ rather than ‘seeped’ fluids.

Response: done.

4) Line 61. Suggest ‘In addition’ to replace ‘On the other hand’, as this is not a contrasting observation.

Response: done.

5) Line 76. ‘Englobes’ is not an English word. Seems like a transliteration of ‘encompasses’.

Response: done.

6) Line 128. Don’t start sentence with a number – spell it out.

Response: done.

7) Line 152. Can the authors give a little more detail of the nature of the samples used for the DNA work. Are these MDACs?

Response: done. We now provide more information on the nature of the samples (lines 155–158 in the revised manuscript).

8) Lines 192-195. The background information about the Gulf of Cadiz isn’t really results and would go better at the start of section 2.

Response: we agree that the background information of the Gulf of Cádiz is not part of results. However, the Pompeia Province region, which our study is focused on, has not been described in detail so far. We here provide the first description of geological structures in this area (Southern and Northern Pompeia Coral ridges, Cold-water Coral Mounds Fields), including novel data (e.g., bathymetry, seismics). For this reason, we consider it appropriate to report these findings in the results sections.

9) Line 241 and other places. It’s quite difficult at the moment to correlate the isotopic

data in Table 2 with the sample points in Figure 7, because the specimen images in Figure 7 are not quite large enough to distinguish samples of authigenic carbonates from embedded coral skeletons. Therefore, could the authors add a column into Table 2 that makes it clear what the samples are for each of the isotopic data points, e.g. authigenic carbonate or coral skeleton.

Response: done. One more column has been added in Table 2 as proposed, indicating the type of samples from which stable isotopic analyses are.

10) Line 253. Replace ‘stems’ with ‘comes’.

Response: done.

11) Line 254. In the figure the ‘worms’ look like serpulid worm tubes. Is this so? In which case please add this information.

Response: done.

12) Line 291. Replace ‘On the contrary’ with ‘In contrast’.

Response: done.

13) Line 296. Spell out ‘2D’ at start of sentence.

Response: done.

14) Line 305 and elsewhere. What is ‘dripping-like’ seepage? This isn’t a description I recognize, so it would be helpful if the authors specify what this means.

Response: done. “Dripping-like refers to intermittent bubbling fluids” (lines 308–309 in the revised manuscript).

15) Line 317. Suggest ‘data’, rather than ‘evidences’.

Response: done.

16) Line 330. I’m unclear where is being referred to here.

Response: removed.

17) Line 332. ‘appear’, not ‘appears’, as preceding diapirs is plural.

Response: done.

18) Line 339. Typo. Angle not angel.

Response: done.

19) Lines 346-354. The authors here suggest that the seawater-like values of the delta C13 from the dead scleractinian skeletons and those embedded in the MDAC show that the corals do not use

methane as a food source, either directly or through symbionts. The authors need to be careful here, because some seep organisms that demonstrably do use methane (and sulfide) from seep fluids for food via endosymbionts produce carbonate skeletons that also have seawater-like delta C13 signatures. I am referring here to vesicomyid and bathymodiolin bivalves, that sequester seawater bi-carbonate ions to produce their shells. Using this model, having seawater-like delta C13 values in the coral skeletons does not prove that these animals do not use chemosynthetic food sources at the site. Really, to be able to settle this conclusively, authors would have to do isotopic, histological and DNA work on living corals from their site, not just on skeletal material and MDAC. In addition, it would be worth noting that scleractinian corals are found embedded in ancient seep carbonates too (see Goedert and Peckmann 2005); there may be some useful comparative isotopic data in that paper.

Response: We included the paper by Goedert and Peckmann, 2005. We fully agree that analyses of coral tissues ($\delta^{13}\text{C}$, DNA) would add important information on their nutrition and metabolic relationships. However, we still regard $\delta^{13}\text{C}$ values of their skeletons as valuable proxy for the possible uptake of CH_4 . Corals utilize HCO_3^- deriving from both the environment and the internal production of CO_2 for skeleton biomineralization (Swart, 1983; Zoccola et al., 2015; Nakamura et al., 2018). Therefore, if they uptake CH_4 as a carbon source, the CO_2 produced from CH_4 metabolism would be used, and consequently parts of the HCO_3^- utilized for biomineralization would be isotopically depleted. This “mixing effect” would result in at least partially depleted $\delta^{13}\text{C}$ values of the skeletons, similar to some chemosynthetic vesicomyid and lucinid bivalves (Hein et al., 2006). The skeletons of the corals analyzed herein, however, exhibit significantly higher $\delta^{13}\text{C}$ values than the co-occurring AOM-derived carbonates. Thus, they are not indicative for CH_4 as important carbon source.

20) Lines 364-367. The entombment of coral skeletons by MDAC may have no consequence to corals, if they are already dead. It’s not entirely clear from the text if the corals associated with the MDAC are dead or alive. If they are alive then this argument is stronger. Also, in most seep environments MDACs form in the subsurface where AOM reactions are occurring. Is this the case at this site? What proof is there of active MDAC formation at the sediment-water interface, as indicated in Figure 12? This is pertinent to the arguments in section 4.3.

Response: We cannot determine if the scleractinian corals embedded in AOM-derived carbonates (samples D10-R3 and D11-R8) were alive or dead when they were buried. However, we observed living corals in areas that are currently affected by seepage (e.g. the Northern Pompeia Coral Ridge, lines 235–236 in the revised manuscript; Fig. 6, C). Furthermore, we observed living octocorals growing on surfaces of currently formed AOM-derived carbonates (e.g., in an active pockmark in the Al Gacel MV, sample D10-R7; Fig. 5, C). These observations imply that corals in these regions are directly affected by methane seepage and the microbially mediated formation of carbonates due to AOM.

References

Hein, J. R., Normark, W. R., McIntyre, B. R., Lorenson, T. D., and Powell, C. L.: Methanogenic calcite, ^{13}C -depleted bivalve shells, and gas hydrate from a mud volcano offshore southern California, *Geology*, 34(2), 109–112, 2006.

- Nakamura, T., Nadaoka, K., Watanabe, A., Yamamoto, T., Miyajima, T., and Blanco, A. C.: Reef-scale modeling of coral calcification responses to ocean acidification and sea-level rise, *Coral Reefs*, 37, 2018.
- Swart, P. K.: Carbon and Oxygen Isotope Fractionation in Scleractinian Corals: a Review, *Earth-Sci. Rev.*, 19, 51–80, 1983.
- Zoccola, D., Ganot, P., Bertucci, A., Caminit-Segonds, N., Techer, N., Voolstra, C. R., Aranda, M., Tambutté, E., Allemand, D., Casey, J. R., and Tambutté, S.: Bicarbonate transporters in corals point towards a key step in the evolution of cnidarian calcification, *Sci. rep.-UK*, 5, 2015.

Authors response to Referee n° 3

We are thankful for your useful and interesting comments. We hope we have addressed successfully the different issues discussed here.

Main issues

-The authors write that the “This study aims at elucidating the linkage between the present-day formation of MDACs and CWCs development along the Pompeia Province (Fig. 1),”, but it is not clear why the selected analysis is the best way to achieve this. For example, “Petrographic analysis” is described in the Methods but it is not clear why this analysis is necessary to answer the questions addressed in the manuscript. The suspected nutritional linkage between CWC and hydrocarbon seepage is known in the literature as the ‘hydraulic theory’ (see Hovland, Jensen et al. 2012 and references therein). The present study is a direct test of this theory in an area that is very suited to test this. The name “hydraulic theory” and/or related reference are however not mentioned in the manuscript (e.g. ln 50-52)

Response: The “hydraulic theory” is now included in the introduction with references. Petrographic analyses are needed to be sure that these are seep carbonates, and to find the right sampling points for isotope analysis — we have to discriminate between authigenic carbonates, corals, micritic phases. of samples. For instance, embedded corals in some of the AOM-carbonates (D10-R3 and D11-R8) have been described and discriminated from the AOM-carbonate facies by petrographic analysis.

-Another major problem was description of the sampling design and the method of sampling. The authors write on line 84-86 “This study is based on collected data from the Pompeia Province, during the Subvent-2 cruise in 2014 aboard the R/V Sarmiento de Gamboa. The analysed samples were recovered from the Al Gacel MV (D10-R3, D10-R7, D11-R8) and the Northern Pompeia Coral Ridge (D03-B1) (Fig. 1).” This description is grossly inadequate. What was the sampling design? Are ‘samples’ collected ad random or based a preconceived plan? Why those sites? What material was sampled as ‘the samples’ (e.g. living coral pieces, coral rubble, sediment with rubble, carbonates)? Size/weight of the samples? Number of samples? Replication? How are the samples taken (ROV arm, push core)? How were samples stored on the ROV, how long before samples reached the surface how are samples processed/stored on-board (significant given the DNA/RNA analysis, e.g. with respect to cross contamination, microbial community shifts)?

Detailed response to “What was the sampling design? Are ‘samples’ collected ad random or based a preconceived plan? Why those sites? How are the samples taken (ROV arm, push core)? How were samples stored on the ROV, how long before samples reached the surface how are samples processed/stored on-board (significant given the DNA/RNA analysis, e.g. with respect to cross contamination, microbial community shifts)?”: we included more information on the study design, storage and sampling procedure in the material and methods section (see lines 84–92 on the new revised manuscript).

Detailed response to “What material was sampled as ‘the samples’ (e.g. living coral pieces, coral rubble, sediment with rubble, carbonates)? Size/weight of the samples? Number of samples?”

Replication?”: Information about the samples (what is each sample) is detailed in the “Petrography and stable isotopes of carbonates” results (section 3.3). Size of the samples are given with a scale bar in Fig. 7 (A, C, E, F). Weight of the samples was not determined. Each sample is one unit (i. e. coral fragment, carbonate from the based of the Al Gacel MV, carbonate from an active pockmark in Al Gacel MV, and carbonate from the summit of the Al Gacel MV). Replicates used for DNA analysis have been described in section 2.6.1. Furthermore, stable isotopic values obtained from precise sampling sites performed on each sample (section 2.4) are shown in Figure 7 (B, D, F) and Table 2.

The authors are addressing ecological questions (see e.g. line 34-38, line 50-52 and line 75 “...present-day formation of MDACs and CWCs development...”) using studies of carbonates. One of the issues that is particularly relevant for the interpretation of these data is whether the analysis was performed on carbonates with living CWC or not. From the pictures and description, it seems plausible that only dead CWC carbonates were studied (although ln 348 mentions “the necrotic part of living *Madrepora*”), but this begs the question how representative the RNA/DNA/biomarker analysis is when only carbonates of dead CWCs are studied. To what extent do the authors think that the organic components of the carbonates still represent the CWC microbial community? Similarly for the ¹³C carbonate analysis, is it known well enough whether CWCs leave a distinct isotope mark in the carbonates that is representative for feeding on surface derived organic matter versus hydrocarbons? Targeted sampling of also living CWC pieces and comparison with the sampled carbonates would have provided a means to address this.

Response: since the necrotic coral-carbonate (D03-B1) used for environmental DNA analysis belongs to a living *Madrepora oculata*, it is expected that 16S rDNA libraries reveal DNA related to microorganisms related to the corals’ microbiota. For instance, sequences related to Enterobacteria and Verrucomicrobia were found in this sample (Supplementary **Table S1**) and are normally in the environment and found associated with corals and other animals (Sorokin et al., 1995; Webster et al., 2016), while *Nitrosococcus* bacteria are ammonia-oxidizers, probably involved in the regulation of nitrogen cycle of the coral’s holobiont (Rädecker et al., 2015). Thus, we would have found DNA related to chemosynthetic microorganisms in case the coral fed from the seeping fluids.

Furthermore, it has been supported by many that coral-carbonate skeletons do partially reflect corals nutrition, since part of the HCO₃⁻ used for its formation comes from the coral’s metabolism, i. e. CO₂ formed from cellular respiration (Swart, 1983; Zoccola et al., 2015; Nakamura et al., 2018). Thus, stable carbon isotopic analysis is an optimal procedure to observe if corals used methane as a carbon source.

-The authors mention that the ROV had sensors for CO₂ and CH₄ data and could take NISKIN water samples for CH₄. In the results section (ln 219-221 and ln 231) CH₄ data are mentioned but in the M&M nothing can be found on sampling location (e.g. height above sediment), sensor calibration, samples handling, sample analyses of the water samples.

Response: Niskin water analysis were not performed for this study, rather done by colleagues from the Subevent-2 project which have previously published the methane values recovered from the Niskin bottles. Sampling procedure can be found in their publication (Sánchez-Guillamón et al., 2015).

The site description in 3.1 should be partly moved to the Materials and Methods. Only the new results from this study should stay in 3.1.

Response: the Pompeia Province region has been described in detail for the first time in this study. We provide geological structures in this area (Southern and Northern Pompeia Coral ridges, Cold-water Coral Mounds Fields), including novel data (e.g., bathymetry, seismics). Therefore, we consider it appropriate to report these findings in the results sections.

-The authors infer that “severe seepage results in lethal conditions for CWCs” (line 363 - 364 and 377-378), but I see no evidence for that in the paper. In addition, the authors concluded that CWCs can be entombed by MDAC formation, it is however not clear whether this entombment is the cause of CWC mortality or that this entombment took place after CWC demise following for example from post-glacial decrease in current strength.

Response: We cannot determine if the scleractinian corals embedded in AOM-derived carbonates (samples D10-R3 and D11-R8) were alive or dead when they were buried. However, we observed living corals in areas that are currently affected by seepage (e.g. the Northern Pompeia Coral Ridge, lines 236–237 in the revised manuscript; Fig. 6, C). Furthermore, we observed living octocorals growing on surfaces of currently formed AOM-derived carbonates (e.g., in an active pockmark in the Al Gacel MV, sample D10-R7; Fig. 5, C). These observations indicate that CWCs can live when seepage occurs by means of the “buffer effect” (section 4.3) but severe seepage which cannot be completely buffered may end killing the CWCs.

Suggestions for minor edits:

-ln 48-50: reduce number of refs

Response: done.

-ln 59: reduce number of refs

Response: done.

-ln 72-73: reduce number of refs

Response: done.

-ln 112: Please also give the values of the VPDB used, to avoid confusion

Response: done. Please see lines 116–11 of the new revised manuscript.

-ln 124: “have a global distribution” instead of “globally widespread”

Response: done in line 14 of the revised manuscript.

-ln 152: replace “... solid samples were...” with “...sample material was...”

Response: done.

-In 230: replace "...by dead.." with "... by shells of the chemosynthetic bivalves *Lucinoma*..."

Response: done.

-In 243: What does "virtually influenced" mean?

Response: "virtually" was deleted.

-In 262: "... values ranging from...". From the methods it is unclear on what this range is based, replication, multiple samples?

Response: The range is based on the different values obtained along the same petrographic facies of each sample (Figs. 7 & 9; Table 2). The numbers shown on the petrographic sections of each sample in Figure 7 (Fig. 7, B, D, F), indicate the exact sampling points used for stable isotopic analysis, which values are shown in Table 2. Further information has been included in the foot of Fig. 7 to facilitate this information for the readers.

-In 307: What does "proportions" here mean? Do you mean "rates" or "concentrations"?

Response: concentrations. Changed.

-In 308: So was methane sampled upon removal of the carbonate blocks?

Response: yes. Information added in line 320 of the new revised manuscript (see Sánchez-Guillamón et al., 2015 for details).

-In 368: The authors also mentioned the availability of a CO₂ sensor on the ROV. Has this been used to measure aragonite saturation states at the different locations?

Response: The aragonite saturation states influences in the formation of corals skeletons and calcium carbonate precipitation. The CO₂ sensors could only give us qualitative approaches of the presence or absence of CO₂, but not concretely values. Interestingly, Niskin samples revealed high dissolved CO₂ concentrations in Al Gacel MV above the seafloor (Sánchez-Guillamón et al., 2015), what complicates the precipitation of calcium carbonate. Further measurements are needed to approach the aragonite saturation state of the different locations.

-In 755: Fig 4C. There is a black pointing to "octocorals", but I cannot see these on the picture.

Response: they are on top of the carbonate, difficult to observed since they are semi-transparent. Figure was improved.

References

- Nakamura, T., Nadaoka, K., Watanabe, A., Yamamoto, T., Miyajima, T., and Blanco, A. C.: Reef-scale modeling of coral calcification responses to ocean acidification and sea-level rise, *Coral Reefs*, 37, 2018.
- Rädecker, N., Pogoreutz, C., Voolstra, C. R., Wiedenmann, J., and Wild, C: Nitrogen cycling in corals: The key to understanding holobiont functioning?, *Trends Microbiol.*, 23(8), 490–497, 2015.
- Sánchez-Guillamón, O., García, M. C., Moya-Ruiz, F., Vázquez, J. T., Palomino, D., Fernández-Puga, M. C., and Sierra, A.: A preliminary characterization of greenhouse gas (CH₄ and CO₂) emissions from Gulf of Cádiz mud volcanoes, VIII Symposium MIA15, 2015.
- Sorokin, Y. I.: *Coral reef ecology*. Vol. 102, Springer Science & Business Media, 1995.
- Swart, P. K.: Carbon and Oxygen Isotope Fractionation in Scleractinian Corals: a Review, *Earth-Sci. Rev.*, 19, 51–80, 1983.
- Webster, N. S., Negri, A. P., Botté, E. S., Laffy, P. W., Flores, F., Noonan, S., ... and Uthicke, S.: Host-associated coral reef microbes respond to the cumulative pressures of ocean warming and ocean acidification, *Scientific reports*, 6, 19324, 2016.
- Zoccola, D. Ganot, P., Bertucci, A., Caminit-Segonds, N., Techer, N., Voolstra, C. R., Aranda, M., Tambutté, E., Allemand, D., Casey, J. R., and Tambutté, S.: Bicarbonate transporters in corals point towards a key step in the evolution of cnidarian calcification, *Sci. rep.-UK*, 5, 2015.

Authors additional minor modifications

- 1) Line 3: Francisco Javier González instead of Javier González.
- 2) Line 55: “in northern Rockall Trough”.
- 3) Line 61: citation Goedert & Peckmann, 2005 added.
- 4) Line 65: “with only a few living corals”.
- 5) Line 269 – 270: change the position of the references to Fig. 4, D and add the reference to Fig. 7, E.
- 6) Line 275: deleted “and the acyclic isoprenoid hop-17(21)-ene.”.
- 7) Line 277: changed from “C₂₈” to “C₃₃” and from “n-C₂₈” to “n-C₃₁”.
- 8) Line 282: changed from “ $\Delta^{13}\text{C}$ ” to “ $\delta^{13}\text{C}$ ”.
- 9) Line 284: 3.5. Section title changed to “Prokaryotic community structure”.
- 10) Line 308 – 309: adding clarification of what dripping-like means.
- 11) Line 337: “with varying”.
- 12) Line 395 – 405: minor changes on the structure of the text.
- 13) Line 421: “Francisco Javier González”.
- 14) Line 491–493: Reference of Goedert & Peckmann, 2005
- 15) Line 752: “in northern Pompeia Province” not “in the northern Pompeia Province”.
- 16) Line 754: “ultra-high seismic profile” and “Northern Pompeia Coral Ridge”.
- 17) Line 757: “Ultra-high resolution (A) and multichannel (B) seismic profiles” and “in southern Pompeia Province” not “in the southern Pompeia Province”.
- 18) Line 762: “active pockmark sites”.
- 19) Line 769: “active pockmark site”.
- 20) Line 776 – 777: added “where there is currently a diffused seepage of fluids”.
- 21) Line 810: “Bar charts representing relative abundances of prokaryotic taxa detected in each sample”.
- 22) Figure 10 modified. Some annotations needed to be corrected.
- 23) Figure 11 modified. Adding information about the sample as requested from Referee n° 1.

Cold-water corals and hydrocarbon-rich seepage in the Pompeia Province (Gulf of Cádiz) — living on the edge

Blanca Rincón-Tomás¹, Jan-Peter Duda^{2,3}, Luis Somoza⁴, ~~Francisco~~ Javier González⁴, Dominik Schneider¹, Teresa Medialdea⁴, Pedro Madureira⁵, Michael Hoppert¹, and Joachim Reitner^{2,3}

¹Georg-August-University Göttingen, Institute of Microbiology and Genetics, Grisebachstraße 8, 37077 Göttingen, Germany

²Georg-August-University Göttingen, Göttingen Centre of Geosciences, Goldschmidtstraße 3, 37077 Göttingen, Germany

³Göttingen Academy of Sciences and Humanities, Theaterstraße 7, 37073 Göttingen, Germany

⁴Marine Geology Dept., Geological Survey of Spain, IGME, Ríos Rosas 23, 28003 Madrid, Spain

⁵Estrutura de Missão para a Extensão da Plataforma Continental. Rua Costa Pinto 165, 2770-047 Paço de Arcos, Portugal

Correspondence to: Blanca Rincón-Tomás (b.rincontomas@gmail.com)

Abstract. Azooxanthellate cold-water corals (CWCs) ~~have a global distribution are globally widespread~~ and have commonly been found in areas of active fluid seepage. The relationship between the CWCs and these fluids, however, is not well understood. This study aims at unravelling the relationship between CWC development and hydrocarbon-rich seepage in the Pompeia Province (Gulf of Cádiz, Atlantic Ocean). This region comprises mud volcanoes, coral ridges and fields of coral mounds, which are all affected by the tectonically driven seepage of hydrocarbon-rich fluids. ~~The type of seepage such as focused, scattered, diffused or eruptive~~ ~~Rate and type of seepage (i.e. focused, scattered, diffused, eruptive)~~, however, is tightly controlled by a complex system of faults and diapirs. Early diagenetic carbonates from the currently active Al Gacel MV exhibit $\delta^{13}\text{C}$ -signatures down to -28.77‰ VPDB, indicating biologically derived methane as the main carbon source. The same samples contained ^{13}C -depleted lipid biomarkers diagnostic for archaea such as crocetane ($\delta^{13}\text{C}$ down to -101.2‰ VPDB) and PMI ($\delta^{13}\text{C}$ down to -102.9‰ VPDB), evidencing microbially mediated anaerobic oxidation of methane (AOM). This is further supported by next generation DNA sequencing data, demonstrating the presence of AOM related microorganisms (ANME archaea, sulfate-reducing bacteria) in the carbonate. Embedded corals in some of the carbonates and CWC fragments exhibit less negative $\delta^{13}\text{C}$ values (-8.08 to -1.39‰ VPDB), pointing against the use of methane as ~~the~~ carbon source. Likewise, the absence of DNA from methane- and sulfide-oxidizing microbes in a sampled coral does not support a chemosynthetic lifestyle of these organisms. In the light of these findings, it appears that the CWCs benefit rather indirectly from hydrocarbon-rich seepage by using methane-derived authigenic carbonates as ~~a~~ substratum for colonization. At the same time, chemosynthetic organisms at active sites prevent coral dissolution and necrosis by feeding on the ~~seeped-seeping~~ fluids (i. e. methane, sulfate, hydrogen sulfide), allowing cold-water corals to colonize carbonates currently affected by hydrocarbon-rich seepage.

1. Introduction

Cold-water corals (CWCs) are a widespread, non-phylogenetic group of cnidarians ~~which-that~~ include hard skeleton scleractinian corals, soft-tissue octocorals, gold corals, black corals and hydrocorals (Roberts et al., 2006; Roberts et al., 2009; Cordes et al., 2016). ~~Typically, they thrive at low temperatures (4 – 12 °C). They typically thrive at low temperatures (4 – 12 °C)~~ and occur in water depths of ca. 50 – 4000 m. CWCs are azooxanthellate

39 and solely rely on their nutrition as energy and carbon sources (Roberts et al., 2009). -Some scleractinian corals
40 (e.g. *Lophelia pertusa*, *Madrepora oculata*, *Dendrophyllia cornigera*, *Dendrophyllia alternata*, *Eguchipsammia*
41 *cornucopia*) are able to form colonies or even large carbonate mounds (Rogers et al., 1999; Wienberg et al., 2009;
42 Watling et al., 2011; Somoza et al., 2014). Large vertical mounds and elongated ridges formed by episodic growth
43 of scleractinian corals (mainly *Lophelia pertusa*) are for instance widely distributed along the continental margins
44 of the Atlantic Ocean (Roberts et al., 2009). -These systems are of great ecological value since they offer sites for
45 resting-, breeding-, and feeding for various invertebrates and fishes (Cordes et al., 2016 and references therein).
46 ~~Several environmental forces influence the initial settling, growth, and decline of CWCs. Several ecological forces~~
47 ~~are discussed to control the initial settling, growth, and decline of CWCs.~~ These include, among others, an
48 availability of suitable substrates for coral larvae settlement, low sedimentation rates, oceanographic boundary
49 conditions (e.g. salinity, temperature and density of the ocean water) and a sufficient supply of nutrients through
50 topographically controlled currents systems (Mortensen et al., 2001; Roberts et al., 2003; Thiem et al., 2006;
51 Dorschel et al., 2007; Dullo et al., 2008; Van Rooij et al., 2011; Hebbeln et al., 2016)(e.g. ~~Freiwald et al., 1999;~~
52 ~~2002; Mortensen et al., 2001; Roberts et al., 2003; Thiem et al., 2006; Dorschel et al., 2007; Dullo et al., 2008;~~
53 ~~Frank et al., 2011; Van Rooij et al., 2011; Hebbeln et al., 2016).~~- Alternatively, the “hydraulic theory” supports
54 ~~that CWC~~ ecosystems may be directly fueled by fluid seepage, providing a source of e.g. sulfur compounds,
55 nitrogen compounds, P, CO₂ and/or hydrocarbons (Hovland, 1990; Hovland and Thomsen, 1997; Hovland et al.,
56 1998; 2012). This relationship is supported by the common co-occurrence of CWC-mounds and hydrocarbon-rich
57 seeps around the world, ~~for example as e.g.~~ at the Hikurangi Margin in New Zealand (Liebetrau et al., 2010), the
58 Brazil margin (e.g. Gomes-Sumida et al., 2004), the Darwin Mounds in the northern Rockall Trough (Huvette et
59 al., 2009), the Kristin field on the Norwegian shelf (Hovland et al., 2012), the western Alborán Sea (Margreth
60 et al., 2011), and the Gulf of Cádiz (e.g. Díaz-del-Río et al., 2003; Foubert et al., 2008). However, CWCs may also
61 benefit rather indirectly from seepage. For instance, methane-derived authigenic carbonates (MDACs) formed
62 through the microbially mediated anaerobic oxidation of methane (AOM; ~~Suess & Whiticar, 1989; Hinrichs et al.,~~
63 ~~1999; Thiel et al., 1999; Boetius et al., 2000; Hinrichs & Boetius, 2002~~~~Suess & Whiticar, 1989; Hinrichs et al.,~~
64 ~~1999; Thiel et al., 1999; Boetius et al., 2000; Hinrichs & Boetius, 2002; Valentine, 2002; Boetius & Suess, 2004)~~
65 potentially provide hard substrata for larval settlement (e.g. Díaz-del-Río et al., 2003; Van Rooij et al., 2011;
66 Magalhães et al. 2012; Le Bris et al., 2016; Rueda et al., 2016). ~~In addition~~~~On the other hand~~, larger hydrocarbon-
67 rich seepage related structures such as mud volcanoes and carbonate mud mounds act as morphological barriers
68 favoring turbulent water currents that deliver nutrients to the corals (Roberts et al., 2009; Wienberg et al., 2009;
69 Margreth et al., 2011; Vadorpe et al., 2016).
70 In the Gulf of Cádiz, most CWC occurrences are “coral graveyards” ~~with only a few living corals (i.e., with only~~
71 ~~few living corals)~~ that are situated along the Iberian and Moroccan margins. These CWC systems are typically
72 associated with diapiric ridges, steep fault-controlled escarpments, and mud volcanoes (MVs) such as the Faro
73 MV, Hesperides MV, Mekness MV, and MVs in the Pen Duick Mud Volcano Province (Foubert et al., 2008;
74 Wienberg et al., 2009). MVs (and other conspicuous morphological structures in this region such as pockmarks)
75 are formed through tectonically induced fluid flow (Pinheiro et al., 2003; Somoza et al., 2003; Medialdea et al.,
76 2009; León et al., 2010; 2012). This is because of the high regional tectonic activity and high fluid contents of
77 sediments in this area (mainly CH₄ and, to a lesser extent, H₂S, CO₂, and N₂; Pinheiro et al., 2003; Hensen et al.,
78 2007; Scholz et al., 2009; Smith et al., 2010; González et al., 2012). However, the exact influence of fluid flow on
79 CWC growth in this region remains elusive.

80 This study aims at elucidating the linkage between the present-day formation of MDACs and CWCs development
81 along the Pompeia Province (Fig. 1), which ~~encompasses englobes~~ mud volcanoes as the Al Gacel MV (León et
82 al., 2012), diapiric coral ridges and mounds. We address this question by the combined analyses of high-resolution
83 ROV underwater images, geophysical data (e.g. seabed topography, deep high-resolution multichannel seismic
84 reflection data), and sample materials (petrographic features, $\delta^{13}\text{C}$ - and $\delta^{18}\text{O}$ -signatures of carbonates, lipid
85 biomarkers and environmental 16s rDNA sequences of the prokaryotic microbial community). Based on our
86 findings, we propose an integrated model to explain the tempo-spatial and genetic relations between CWCs,
87 chemosynthetic fauna and hydrocarbon-rich seepage in the study area.

88 2. Materials and Methods

89 ~~This study is based on data and samples from the Pompeia Province that were collected during the Subvent-2~~
90 ~~cruise in 2014 aboard the R/V Sarmiento de Gamboa (Fig. 1). In order to elucidate the tempo-spatial and genetic~~
91 ~~relations between CWCs, chemosynthetic fauna and hydrocarbon-rich seepage in this area, we explored geological~~
92 ~~features by means of underwater imaging and geophysical data. Based on these findings, we sampled different~~
93 ~~geological structures (mud volcanoes and coral ridges). All samples were taken with a ROV arm and immediately~~
94 ~~stored at room temperature (petrographic analysis), -20 degrees (stable isotopic analysis), and -80 degrees~~
95 ~~(environmental DNA analysis). Subsequently, we conducted detailed analyses on selected sample materials from~~
96 ~~sites that were characterized by different types of seepage during sampling. These include sites at the Al Gacel~~
97 ~~MV (D10-R3, D10-R7, D11-R8) and the Northern Pompeia Coral Ridge (D03-B1) (Fig. 1). This study is based on~~
98 ~~collected data from the Pompeia Province, during the Subvent 2 cruise in 2014 aboard the R/V Sarmiento de~~
99 ~~Gamboa. The analyzed samples were recovered from the Al Gacel MV (D10 R3, D10 R7, D11 R8) and the~~
100 ~~Northern Pompeia Coral Ridge (D03 B1) (Fig. 1).~~

101 2.1. Geophysical survey

102 Seabed topography of the studied sites was mapped by using an Atlas Hydrosweep DS (15 kHz and 320 beams)
103 multibeam echosounder (MBES). Simultaneously, ultra-high resolution sub-bottom profiles were acquired with
104 an Atlas Parasound P-35 parametric chirp profiler (0.5 – 6 kHz). Deep high-resolution multichannel seismic
105 reflection data was obtained using an array of 7 SERCEL gi-guns (system composed of 250 + 150 + 110 + 45
106 cubic inches) with a total of 860 cubic inches. The obtained data were recorded with an active streamer
107 (SIG@16.3x40.175; 150 m length with 3 sections of 40 hydrophones each). The shot interval was 6 seconds and
108 the recording length 5 seconds two-way travel time (TWT). Data processing (filtering and stacking) was performed
109 on board with Hot Shots software.

110 2.2. Video survey and analysis

111 A remotely operated vehicle (ROV-6000 Luso) was used for photographic documentation (high definition digital
112 camera, 1024x1024 pixel) and sampling. The ROV was further equipped with a STD/CTD-SD204 sensor (*in-situ*
113 measurements of salinity, temperature, oxygen, conductivity, sound velocity and depth), HydroCTM sensors (*in-*
114 *situ* measurements of CO₂ and CH₄) and Niskin bottles (CH₄ concentrations).

115 2.3. Petrographic analysis

116 General petrographic analysis was performed on thin sections (ca. 60 µm thickness) with a Zeiss SteREO
117 Discovery.V8 stereomicroscope (transmitted- and reflected light) linked to an AxioCam MRc 5-megapixel camera.
118 Additional detailed petrographic analysis of textural and mineralogical features was conducted on polished thin
119 sections (ca. 30 µm thickness) using a DM2700P Leica Microscope coupled to a DFC550 digital camera.
120 Carbonate textures have been classified following Dunham (1962) and Embry & Klovan (1971).

121 **2.4. Stable isotopes ($\delta^{13}\text{C}$, $\delta^{18}\text{O}$) of carbonates**

122 Stable carbon and oxygen isotope measurements were conducted on ca. 0.7 mg carbonate powder obtained with a
123 high precision drill (\varnothing 0.8 mm). The analyses were performed with a Thermo Scientific Kiel IV carbonate device
124 coupled to a Finnigan Delta Plus gas isotope mass spectrometer. ~~Accuracy and reproducibility were checked~~
125 ~~through the replicate analysis of a standard (NBS19) and reproducibility was better than 0.1 ‰. Stable carbon and~~
126 ~~oxygen isotope values are expressed in the standard δ notation as per mill (‰) deviations relative to Vienna Pee~~
127 ~~Dee Belemnite (VPDB) Reproducibility was checked through the replicate analysis of a standard (NBS19) and was~~
128 ~~generally better than 0.1 ‰. Stable carbon and oxygen isotope values are expressed in the standard δ notation as~~
129 ~~per mill (‰) deviations relative to Vienna Pee Dee Belemnite (VPDB).~~

130 **2.5. Lipid biomarker analysis**

131 **2.5.1. Sample preparation**

132 All materials used were pre-combusted (500 °C for >3 h) and/or extensively rinsed with acetone prior to sample
133 contact. A laboratory blank (pre-combusted sea sand) was prepared and analyzed in parallel to monitor laboratory
134 contaminations.

135 The preparation and extraction of lipid biomarkers was conducted in orientation to descriptions in Birgel et al.
136 (2006). Briefly, the samples were first carefully crushed with a hammer and internal parts were powdered with a
137 pebble mill (Retsch MM 301, Haan, Germany). Hydrochloric acid (HCl; 10 %) was slowly poured on the powdered
138 samples which were covered with dichloromethane (DCM)-cleaned water. After 24 h of reaction, the residues (pH
139 3 – 5) were repeatedly washed with water and then lyophilized.

140 3 g of each residue was saponified with potassium hydroxide (KOH; 6 %) in methanol (MeOH). The residues were
141 then extracted with methanol (40 mL, 2x) and, upon treatment with HCl (10 %) to pH 1, in DCM (40 mL, 2x) by
142 using ultra-sonification. The combined supernatants were partitioned in DCM vs. water (3x). The total organic
143 extracts (TOEs) were dried with sodium sulfate (NaSO_4) and evaporated with a gentle stream of N_2 to reduce loss
144 of low-boiling compounds (cf. Ahmed and George, 2004).

145 ~~Fifty percent~~50 % of each TOE was separated over a silica gel column (0.7 g Merck silica gel 60 conditioned with
146 *n*-hexane; 1.5 cm i.d., 8 cm length) into (a) hydrocarbon (6 mL *n*-hexane), (b) alcohol (7 mL DCM/acetone, 9:1,
147 v:v) and (c) carboxylic acid fractions (DCM/MeOH, 3:1, v:v). Only the hydrocarbons were subjected to gas
148 chromatography–mass spectrometry (GC-MS).

149 **2.5.2. Gas chromatography–mass spectrometry (GC-MS)**

150 Lipid biomarker analyses of the hydrocarbon fraction were performed with a Thermo Scientific Trace 1310 GC
151 coupled to a Thermo Scientific Quantum XLS Ultra MS. The GC was equipped with a capillary column
152 (Phenomenex Zebron ZB-5MS, 30 m length, 250 µm inner diameter, 0.25 µm film thickness). Fractions were

153 injected into a splitless injector and transferred to the column at 300 °C. The carrier gas was He at a flow rate of
154 1.5 mL min⁻¹. The GC oven temperature was ramped from 80°C (1 min) to 310 °C at 5 °C min⁻¹ (held for 20 min).
155 Electron ionization mass spectra were recorded in full scan mode at an electron energy of 70 eV with a mass range
156 of m/z 50 – 600 and scan time of 0.42 s. Identification of individual compounds was based on comparison of mass
157 spectra and GC retention times with published data and reference compounds.

158 2.5.3 Gas chromatography–combustion–isotope ratio mass spectrometer (GC-C-IRMS)

159 Compound specific δ¹³C analyses were conducted with a Trace GC coupled to a Delta Plus IRMS via a
160 combustion-interface (all Thermo Scientific). The combustion reactor contained CuO, Ni and Pt and was operated
161 at 940°C. The GC was equipped with two serially linked capillary columns (Agilent DB-5 and DB-1; each 30 m
162 length, 250 μm inner diameter, 0.25 μm film thickness). Fractions were injected into a splitless injector and
163 transferred to the GC column at 290°C. The carrier gas was He at a flow rate of 20 ml min⁻¹. The temperature
164 program was identical to the one used for GC-MS (see above). CO₂ with known δ¹³C value was used for internal
165 calibration. Instrument precision was checked using a mixture of *n*-alkanes with known isotopic composition.
166 Carbon isotope ratios are expressed as δ¹³C (‰) relative to VPDB.

167 2.6. Amplicon sequencing of 16S rRNA genes

168 2.6.1. DNA extraction and 16S rRNA gene amplification

169 [Environmental DNA analyses of microbial communities were performed on a carbonate sample with embedded](#)
170 [corals from the base of the Al Gacel MV \(D10-R3\), a carbonate sample from an active pockmark close to the](#)
171 [summit of the Al Gacel MV \(D10-R7\), and a necrotic fragment of a living *Madrepora oculata* recovered from the](#)
172 [Northern Pompeia Coral Ridge \(D03-B1\).](#) About 1 – 4 g of solid samples were first mashed with mortar and liquid
173 nitrogen to fine powder. Three biological replicates were used per sample. Total DNA was isolated with a Power
174 Soil DNA Extraction Kit (MO BIO Laboratories, Carlsbad, CA). All steps were performed according to the
175 manufacturer's instructions.

176 Bacterial amplicons of the V3 – V4 region were generated with the primer set MiSeq_Bacteria_V3_forward
177 primer (5'-TCGTCGGCAGCGTCAGATGTGTATAAGAGACAGCCTACGGGNGGCWGCAG-3') and
178 MiSeq_Bacteria_V4_reverse primer (5'-
179 GTCTCGTGGGCTCGGAGATGTGTATAAGAGACAGGACTACHVGGGTATCTAATCC-3'). Likewise,
180 archaeal amplicons of the V3 – V4 region were generated with the primer set MiSeq_Archaea_V3_forward primer
181 (5'-TCGTCGGCAGCGTCAGATGTGTATAAGAGACAG-GGTGBCAGCCGCGGTAA-3') and
182 MiSeq_Archaea_V4_reverse primer (5'-GTCTCGTGGGCTCGGAGATGTGTATAAGAGACAG-
183 CCCGCAATYCTTTAAG-3'). 50 μl of the PCR reaction mixture for bacterial DNA amplification, contained
184 1 U Phusion high fidelity DNA polymerase (Biozym Scientific, Oldendorf, Germany), 5% DMSO, 0.2 mM of
185 each primer, 200 μM dNTP, 0.15 μl of 25 mM MgCl₂, and 25 ng of isolated DNA. The PCR protocol for bacterial
186 DNA amplification included (i) initial denaturation for 1 min at 98 °C, (ii) 25 cycles of 45 s at 98 °C, 45 s at 60 °C,
187 and 30 s at 72 °C, and (iii) a final extension at 72 °C for 5 min. The PCR reaction mixture for archaeal DNA
188 amplification was similarly prepared but contained instead 1 μl of 25 mM MgCl₂ and 50 ng of isolated DNA. The
189 PCR protocol for archaeal DNA amplification included (i) initial denaturation for 1 min at 98 °C, (ii) 10 cycles of

190 45 s at 98 °C, 45 s at 63 °C, and 30 s at 72 °C, (iii) 15 cycles of 45 s at 98 °C, 45 s at 53 °C, and 30 s at 72 °C, and
191 (iv) a final extension at 72 °C for 5 min.
192 PCR products were checked by agarose gel electrophoresis and purified using the GeneRead Size Selection Kit
193 (QIAGEN GmbH, Hilden, Germany).

194 **2.6.2. Data analysis and pipeline**

195 Illumina PE sequencing of the amplicons and further process of the sequence data were performed in the Göttingen
196 Genomics Laboratory (Göttingen, Germany). After Illumina MiSeq processing, sequences were analyzed as
197 described in Egelkamp et al. (2017) with minor modifications. In brief, paired-end sequences were merged using
198 PEAR v0.9.10 (Zhang et al., 2014), sequences with an average quality score below 20 and containing unresolved
199 bases were removed with QIIME 1.9.1 (Caporaso et al., 2010). Non-clipped reverse and forward primer sequences
200 were removed by employing cutadapt 1.15 (Martin, 2011). USEARCH version 9.2.64 was used following the
201 UNOISE pipeline (Edgar, 2010). In detail, reads shorter than 380 bp were removed, dereplicated, and denoised
202 with the UNOISE2 algorithm of USEARCH resulting in amplicon sequence variants (ASVs) (Callahan et al.,
203 2017). Additionally, chimeric sequences were removed using UCHIME2 in reference mode against the SILVA
204 SSU database release 132 (Yilmaz et al., 2014). Merged paired-end reads were mapped to chimera-free ASVs and
205 an abundance table was created using USEARCH. Taxonomic classification of ASVs was performed with BLAST
206 against the SILVA database 132. Extrinsic domain ASVs, chloroplasts, and unclassified ASVs were removed from
207 the dataset. Sample comparisons were performed at same surveying effort, utilizing the lowest number of
208 sequences by random subsampling (20,290 reads for bacteria, 13,900 reads for archaea).
209 The paired-end reads of the 16S rRNA gene sequencing were deposited in the National Center for Biotechnology
210 Information (NCBI) in the Sequence Read Archive SRP156750.

211 **3. Results**

212 **3.1. The Pompeia Province — geological settings**

213 The Pompeia Province is situated in the Gulf of Cádiz offshore Morocco, within the so-called Middle Moroccan
214 Field (Ivanov et al., 2000) at water-depths between 860 and 1000 m (**Fig. 1**). It comprises the active Al Gacel
215 MV (**Fig. 1, C**), another mud volcano which is extinct (further referred as extinct MV) and two east-west elongated
216 ridges (Northern Pompeia Coral Ridge and Southern Pompeia Coral Ridge). Scattered coral-mounds surround the
217 ridges with a smooth relief (**Fig. 1, B**). CWCs were observed on seismic profiles resting on all these morphological
218 features. Detailed geological profiles and 3D images of these features are shown in **Figs. 2** and **3**.

219 The Al Gacel MV is a cone-shape structure, 107 m high and 944 m wide, with its summit at 762 m depth and
220 surrounded by a 11 m deep rimmed depression (León et al., 2012) (**Fig. 1, C**). It is directly adjacent to the Northern
221 Pompeia Coral Ridge (**Fig. 2, A–B**), which extends ca. 4 km in westward direction (**Fig. 2, A–B**) and it is
222 terminated by the Pompeia Escarpment (**Fig. 1, B; Fig. 2, C**). High resolution seismic profiles of the Pompeia
223 Escarpment show CWC build-ups (R1 to R4) with steep lateral scarps of ca. 40 m height (**Fig. 2, C**). This MV is
224 of sub-circular shape and exhibits a crater at its top (**Fig. 2, A–B**).

225 Ultra-high resolution sub-bottom seismic profile crossing the Pompeia Province from northwest (NW) to southeast
226 (SE) (**Fig. 3, A**), shows (i) the Al Gacel MV surrounded by bottom-current deposits, (ii) an up to 130 m high CWC
227 framework, growing on top the Southern Pompeia Coral Ridge, and (iii) semi-buried CWC mounds surrounding

228 the ridge in areas of low relief. These CWC mounds locally form smooth, up to 25 – 30 m high top-rounded reliefs
229 that are exposed, but then taper downward below the seafloor (applying sound speeds of 1750 m/s in recent
230 sediments). Additionally, a multichannel seismic profile following the same track but with higher penetration
231 below the seafloor (**Fig. 3, B**) shows high amplitude reflections inside the Al Gacel cone and enhanced reflections
232 at the top of the diapirs (yellow dotted-line in **Fig. 3, B**), pointing to the occurrence of gas (hydrocarbon)-charged
233 sediments. It furthermore exhibits breaks in seismic continuity and diapiric structures at different depths below the
234 Southern Pompeia Coral Ridge and the Al Gacel MV, evidencing a fault system (**Fig. 3, B**). These tectonic
235 structures may promote the development of overpressure areas (OP in **Fig. 3, B**) and consequent upward fluid flow
236 to the surface.

237 **3.2. ROV observation and measurements**

238 Submersible ROV surveys at the Al Gacel MV (**Fig. 1, C**) revealed the presence of dispersed pockmark
239 depressions at the eastern (Dive 10, 790 m) and northern flanks (Dive 11, 760 – 825 m depth). These sites are
240 characterized by focused but low intensity seafloor bubbling (e.g. **Fig. 4, B; Fig. 5, A**). Analysis of water samples
241 revealed CH₄-concentration up to 171 nM during Dive 10 and up to 192 nM during Dive 11 (Sánchez-Guillamón
242 et al., 2015). Pockmarks were essentially formed by grey-olive mud breccia sediments and characterized by
243 deposits of authigenic carbonates appearing in the center and edges, together with typical methane-seep related
244 organisms (e.g. sulfide-oxidizing bacterial mats, chemosynthetic bivalves, siboglinid tubeworms) (**Fig. 4, B–C;**
245 **Fig. 5**). Communities of non-chemosynthetic organisms (e.g. sponges, corals) were also found at pockmarks (**Fig.**
246 **4, B–C; Fig. 5, C**), but were more abundant in places where no seepage was detected (**Fig. 4, A**).
247 Observations with the submersible ROV at the Northern Pompeia Coral Ridge and the extinct MV (Dive 03)
248 revealed widespread and abundant occurrences of dead scleractinian-corals (mainly *Madrepora oculata* and
249 *Lophelia pertusa*) currently colonized by few [living](#) non-chemosynthetic organisms (e.g. *Corallium tricolor*, other
250 octocorals, sea urchins) (**Fig. 6, B–D**). Locally, grey-black colored patches of sulfide-oxidizing bacterial mats
251 surrounded by dead chemosynthetic bivalves (*Lucinoma asapheus* and *Thysira vulcolutre*) were detected (**Fig. 6,**
252 **A**). CH₄-seepage appeared to be less than at the Al Gacel MV, with concentrations of 80 – 83 nM.
253 Water parameters display homogenous values between the four sampling sites (10 °C temperature, ca. 52 – 55 %
254 dissolved oxygen, ca. 31 Kg/m³ density) (**Table 1**).

255 **3.3. Petrography and stable isotopes signatures of carbonates (δ¹⁸O, δ¹³C)**

256 Sample D10-R3 derives from a field of carbonates at the base of the Al Gacel MV which is inhabited by sponges
257 and corals (**Fig. 4, A**). The sample is a frammestone composed of deep water scleractinian corals (*Madrepora* and
258 rare *Lophelia*) (**Fig. 7, A–B**). The corals are typically cemented by microbial automicrite (*sensu* Reitner et al.
259 1995) followed by multiple generations of aragonite. A matrix of dark allomicrite (*sensu* Reitner et al. 1995) with
260 oxidized framboidal pyrites and remains of planktonic foraminifera is restricted to few bioerosional cavities (ca.
261 5%) in the skeletons of dead corals (**Fig. 8, A–B**). δ¹³C signatures of the matrix and cements range from –26.68 to
262 –18.38 ‰, while the embedded coral fragments exhibit δ¹³C values between –5.58 and –2.09 ‰ (**Fig. 7, B; Table**
263 **2**). The δ¹⁸O values generally range from +2.35 to +3.92 ‰ (**Fig. 9; Table 2**).
264 Sample D10-R7 was recovered from a pockmark on the eastern site of the Al Gacel MV that is virtually influenced
265 by active seepage (**Fig. 3, C**). It consists of black carbonate and exhibits a strong hydrogen sulfide (H₂S) odor (**Fig.**
266 **5, B; Fig. 7, C–D**). The top of this sample was inhabited by living octocorals (**Fig. 5, C**), while chemosymbiotic

267 siboglinid worms were present on the lower surface (Fig. 5, D). The sample is characterized by a grey peloidal
268 wackestone texture consisting of allomicrite with abundant planktonic foraminifers and few deep water miliolids.
269 The sample furthermore exhibits some fractured areas which are partly filled by granular and small fibrous cement,
270 probably consisting of Mg-calcite. Locally, light brownish crusts of microbial automicrite similar to ones in D10-
271 R3 are present (see above). Framboidal pyrite is abundant and often arranged in aggregates (Fig. 8, C–D). The
272 carbonate exhibits $\delta^{13}\text{C}$ values ranging from -28.77 to -21.13 ‰ and $\delta^{18}\text{O}$ values from $+2.37$ to $+3.15$ ‰ (Fig. 9;
273 Table 2).

274 Sample D11-R8 stems from an area with meter-sized carbonate blocks at the summit of the Al Gacel MV
275 and is mainly colonized by sponges and serpulid worms (Fig. 4, D). The sample generally exhibits a light grey
276 mud- to wackestone texture consisting of allomicrite with few scleractinian-coral fragments and planktonic
277 foraminifers (Fig. 7, E–F). The carbonate furthermore contains abundant quartz silt and, locally, pyrite
278 enrichments. A further prominent feature are voids that are encircled by dark grey halos and exhibit brownish
279 margins (due to enrichments of very small pyrite crystals and organic matter, respectively). $\delta^{13}\text{C}$ signatures of the
280 matrix and cements range from -14.82 to -14.74 ‰, while embedded coral fragments exhibit $\delta^{13}\text{C}$ values of -4.91
281 to -2.99 ‰ (Fig. 7, F; Table 2). $\delta^{18}\text{O}$ values generally range from $+1.49$ to $+5.60$ ‰ (Fig. 9; Table 2).

282 Sample D03-B1 is a necrotic fragment of a living scleractinian coral (*Madrepora oculata*) recovered from the
283 Northern Pompeia Coral Ridge (Fig. 6, D; Fig. 7, G). The coral-carbonate exhibits $\delta^{13}\text{C}$ values ranging from -8.08
284 to -1.39 ‰ and $\delta^{18}\text{O}$ values from -0.31 to $+2.26$ ‰ (Fig. 9; Table 2).

285 3.4. Lipid biomarkers and compound specific carbon isotope signatures

286 The hydrocarbon fractions of the carbonate recovered from the active pockmark (D10-R7) of the sample D10-R7
287 mainly consist of the irregular, tail-to-tail linked acyclic isoprenoids 2,6,11,15-tetramethylhexadecane (C_{20} ;
288 crocetane), 2,6,10,15,19-pentamethylcosane (C_{25} ; PMI), as well as of several unsaturated homologues of these
289 compounds (Fig. 10). Additionally, it contains the regular, head-to-tail linked acyclic isoprenoid pristane (C_{19})
290 and the cyclic isoprenoid hop-17(21) ene.

291 The hydrocarbon fraction of the carbonate recovered from the summit of the Al Gacel MV (D11-R8) of sample
292 D11-R8 is dominated by *n*-alkanes with chain-lengths ranging from C_{14} to C_{28} (maxima at *n*- C_{16} and,
293 subordinated, at *n*- C_{20} and *n*- C_{28}) (Fig. 10). The sample further contains pristane, crocetane, the head-to-tail
294 linked acyclic isoprenoid phytane (C_{20}) and traces of PMI.

295 Crocetane and PMI exhibited strongly depleted $\delta^{13}\text{C}$ values in the carbonate from the active pockmark (D10-R7)
296 sample D10-R7 (-101.2 ‰ and -102.9 ‰, respectively), while they showed less depleted $\delta^{13}\text{C}$ values in the carbonate from the
297 volcano (D11-R8) sample D11-R8 (-57.2 ‰ and -74.3 ‰, respectively). $\delta^{13}\text{C}$ values of *n*-alkanes in sample the
298 carbonate D11-R8 (*n*- C_{17-22}) ranged between -30.8 ‰ and -33.0 ‰ (Table 3).

300 3.5. DNA inventories (MiSeq Illumina sequences)

301 Bacterial DNA (Fig. 11, A) from samples D10-R3 (authigenic carbonate, base of the Al Gacel MV) and D03-B1
302 (*Madrepora oculata* fragment, Northern Pompeia Coral Ridge) mainly derives from taxa that typically thrive in
303 the water-column (e. g. Actinobacteria, Acidobacteria, Chloroflexi, Bacteroidetes, Woeseiaceae, Dadabacteria,
304 Kaiserbacteria, Poribacteria, Planctomycetes, Gemmatimonadetes). The sample D10-R3 furthermore contains
305 bacterial DNA of the nitrite-oxidizing bacteria *Nitrospira sp.*, while the sample D03-B1 contains DNA of the

306 bacterial taxa Verrucomicrobia, Enterobacteria, *Nitrosococcus*. Noteworthy, one amplicon sequence variant
307 (ASV_189) with low number of clustered sequences has been found in D03-B1, identified as a methanotrophic
308 symbiont of *Bathymodiolus mauritanicus* (see Rodrigues et al., 2013).
309 Up to 50 % of bacterial DNA in sample D10-R7 (authigenic carbonate, top of the Al Gacel MV) derives from taxa
310 that are commonly associated with fluid seepage and AOM, i.e. sulfide-oxidizing bacteria, sulfate-reducing
311 bacteria (SRB) and methane-oxidizing bacteria. The most abundant are SRB taxa like SEEP-SRB1, SEEP-SRB2,
312 *Desulfatiglans*, *Desulfobulbus* and *Desulfococcus*, which typically form consortia with ANME archaea.
313 Archaeal DNA (**Fig. 11, B**) from samples D10-R3 and D03-B1 mainly consist of *Cenarchaeum sp.*, which
314 represents 70 – 90 %. *Candidatus Nitrosopumilus* is the second most abundant in both samples, representing 5 –
315 20 %. ~~In contrast. On the contrary,~~ around 90 % of archaeal DNA in D10-R7 is related to ANME-1 and ANME-2
316 groups, in good concordance with the relative abundances of SRB DNA.
317 Details of the number of reads per taxa are shown in the supplementary data, **Tables 1 and 2.**

318 4. Discussion

319 4.1. Evidence of hydrocarbon-rich seepage affecting the Pompeia Province

320 ~~Two-dimensional 2D~~ multichannel-seismic images show that the Pompeia Province is affected by fluid expulsion
321 related to compressional diapiric ridges and thrust faults (**Fig. 3, B**), as it has been reported from other areas of the
322 Gulf of Cádiz (Somoza et al., 2003; Van Rensbergen et al., 2005; Medialdea et al., 2009). There seem to be
323 different types of fault-conduit systems that link the overpressure zones (OP) with the seafloor (**Fig. 3, B**),
324 controlling both type and rate of seepage (e.g. eruptive, focused, diffused or dripping-like). ~~Dripping-like refers to~~
325 ~~intermittent bubbling fluids.~~ At the Al Gacel MV, conduits are for instance mainly linked to faults and a dense
326 hydro-fracture network, allowing the migration of hydrocarbon-rich muds from the overpressure zone to the
327 surface. During active episodes, eruptions lead to the formation of mud-breccia flows as observed in gravity cores
328 (e.g. León et al., 2012). During rather dormant episodes, focused and dripping-like seepage predominates, forming
329 pockmark features (**Fig. 4, B**).
330 Currently, the Al Gacel MV is affected by continuous and focused dripping-like seepages. These sites of active
331 seepage are characterized by carbonates that are suspected to be methane-derived (e.g. sample D10-R7, **Fig. 4, B–**
332 **C**). In-situ ROV-measurements ~~and~~ subsequent water sample analysis demonstrated high ~~concentrations~~
333 ~~proportions~~ of CH₄ in fluids that were escaping upon removal of ~~the carbonate D10-R7 from the active pockmark~~
334 ~~the D10-R7 carbonate~~ (171 nM; **Fig. 5, A**) (Sánchez-Guillamón et al., 2015). This association suggests a genetic
335 relationship between hydrocarbon-rich seepage and the carbonate, as also evidenced by the low $\delta^{13}\text{C}$ -values of the
336 carbonates analyzed herein (down to ca. –30 ‰, **Fig. 9; Table 2**). Indeed, the grey peloidal texture of this sample
337 resembles that of AOM-derived automicrites from the Black Sea that are related to micro-seepage of methane (cf.
338 Reitner et al., 2005). The here observed isotopically depleted acyclic isoprenoids such as crocetane and PMI ($\delta^{13}\text{C}$
339 values between ca. –103 and –57‰; **Fig. 10; Table 3**) are typical fingerprints of AOM-associated Archaea
340 (Hinrichs et al., 1999; Thiel et al., 1999, 2001; Peckmann et al., 2001; Peckmann & Thiel, 2004), which is also in
341 good accordance with the high abundance of DNA related to ANME. At the same time, abundant framboidal
342 pyrite in the carbonate (**Fig. 8, C–D**) and SRB-related DNA (**Fig. 11**) evidences microbial sulfate reduction in the
343 environment. ~~All these data clearly demonstrate that the carbonates. All these evidences clearly demonstrate that~~
344 ~~the carbonates~~ have been formed via AOM, fueled by fluids from the underlying mud diapir.

345 Other carbonate samples from the Al Gacel MV (i.e. D10-R3 and D11-R8) probably have also been formed due
346 to AOM as they are also isotopically depleted ($\delta^{13}\text{C}$ values between ca. -25 and -15 ‰, **Fig. 9, Table 2**). However,
347 no active gas bubbling was observed during sampling, even though both samples still contain open voids which
348 could form pathways for a continuous migration of fluids. In fact, several characteristics of these voids (e.g. dark
349 halos formed by pyrite, brownish margins due to organic matter enrichments) are very similar to those of methane-
350 derived carbonate conduits (cf. Reitner et al., 2015). This could imply that the intensity of hydrocarbon-rich
351 seepage and consequently AOM, may have fluctuated through time. The relatively low dominance of crocetane
352 and PMI in [the carbonate D11-R8 from the summit of Al Gacel MV sample D11-R8 \(Fig. 10\)](#), as well as their
353 moderately depleted $\delta^{13}\text{C}$ values (-57.2 ‰ and -74.3 ‰, respectively; **Table 3**), could be due to mixing effects
354 and thus be in good accordance [with](#) varying intensities of AOM in the environment. Also, the presence of only
355 few AOM-related DNA sequences (**Fig. 11**) and partly oxidized pyrites [in the carbonate D10-R3 from the base of](#)
356 [the Al Gacel MV in sample D10-R3 \(Fig. 8, A–B\)](#) are well in line with this scenario. ~~In concert it appears that the~~
357 ~~seepage intensity has indeed been fluctuating.~~

358 There is no evidence for eruptive extrusions of muddy materials at the coral ridges. In the Southern Pompeia Coral
359 Ridge (**Fig. 3**), diapirs appear to rather promote an upward migration of hydrocarbon-rich fluids in a divergent
360 way throughout a more extensive seabed area. This results in a continuous and diffused seepage, which promotes
361 the occurrence of AOM and the formation of MDACs at the base of the ridges, related to the sulphate-methane
362 transition zone (SMTZ) (Boetius et al., 2000; Hinrichs and Boetius, 2002; González et al., 2012a). This is in good
363 accordance with the detection of methane (80 – 83 nM) at the Northern Pompeia Coral Ridge and the presence of
364 sulfide-oxidizing bacterial mats and shells of dead chemosynthetic bivalves at the western part of the ridge (**Fig.**
365 **6, A**). Likewise, the CWC Mounds Field surrounding the Southern Pompeia Coral Ridge (**Fig. 3**) is thoroughly
366 characterized by micro-seeps, due to ascending fluids from OPs through low-angle faults. This type of focused
367 seepage may promote formation of MDAC pavements in deeper layers of the sediments (**Fig. 3**), similar to coral
368 ridges along the Pen Duick Escarpment (Wehrmann et al., 2011). The generation of MDAC-hotspots at sites of
369 such seepage also explain the geometry of the downward tapering cones (**Fig. 3**).

370 4.2. Ecological meaning of hydrocarbon-rich seepage for CWCs

371 Our data suggests contemporaneous micro-seepage and CWC growth in the Pompeia Province (e.g. **Fig. 4, B**).
372 This relationship has also been observed elsewhere, e.g. in North Sea and off Mid Norway (Hovland, 1990;
373 Hovland & Thomsen, 1997), and the Angola margin (Le Guilloux et al., 2009). However, scleractinian fragments
374 recovered from the Al Gacel MV (embedded in carbonates D10-R3 and D11-R8, [from the base and summit of the](#)
375 [volcano, respectively](#)) and the Northern Pompeia Coral Ridge (D03-B1, necrotic part of a living *Madrepora*
376 *oculata*) displayed barely depleted $\delta^{13}\text{C}$ values (ca. -8 to -1 ‰; **Fig. 9; Table 2**), close to the $\delta^{13}\text{C}$ of marine
377 seawater (0 ± 3 ‰, e.g. Hoefs, 2015). This does not support a significant uptake of methane-derived carbon by the
378 CWCs and thus a direct trophic dependency as previously proposed (Hovland, 1990). Furthermore, the only DNA
379 in sample D03-B1 that could be attributed to a potential methanotrophic endosymbiont (ASV_189; Rodrigues et
380 al., 2013) occurred in minor amounts and most likely represents contamination from the environment or during
381 sampling. Taken together, there is no evidence that CWCs in the working area harbor microbial symbionts which
382 potentially could utilize the hydrocarbon-rich fluids. More likely, the CWCs feed on a mixture of phytoplankton,
383 zooplankton and dissolved organic matter as previously proposed for ones in other regions (Kiriakoulakis et al.,
384 2005; Duineveld et al., 2007; Becker et al., 2009; Liebetrau et al., 2010). This is in good accordance with the

385 presence of DNA from various common archaeal and bacterial taxa (e.g. Acidobacteria, Actinobacteria,
386 Candidatus *Nitrosopumilus*, *Cenarchaeum sp.*) and some potential members of the corals' holobiont (e.g.
387 Enterobacteria, Verrucomicrobia, *Nitrosococcus sp.*) (Sorokin, 1995; Rådecker et al., 2015; Webster et al., 2016)
388 in sample D03-B1 (Fig. 11).

389 CWC development and hydrocarbon-rich seepage are consequently linked *via* the formation of MDAC deposits,
390 which provide the hard substrata needed for CWC larval settlement (e.g. Díaz-del-Río et al., 2003; Van Rooij et
391 al., 2011; Magalhães et al., 2012; Le Bris et al., 2016; Rueda et al., 2016). If too severe, however, fluid flow and
392 associated metabolic processes can result in local conditions that are lethal to CWCs (see 4.3). Moreover, AOM
393 fueled by fluid flow can also cause an entombment of the CWCs by MDACs (Wienberg et al., 2009, Wienberg &
394 Titschack, 2015), as observed in D10-R3 and D11-R8 carbonates from the Al Gacel MV (Figs. 7 and 9; Tabs. 2
395 and 3). It is therefore not surprising that large CWC systems in the Pompeia Province are always linked to
396 structures that are affected by rather mild, non-eruptive seepage (i.e. the extinct MV, the coral ridges and the CWC
397 Mound Fields: Figs. 3 and 6). The observation that these systems are in large parts "coral graveyards" (Fig. 6, B–
398 D), similar to other areas in the Gulf of Cádiz (see Foubert et al., 2008; Wienberg et al., 2009), may be explained
399 by a post-glacial decrease in current strength (Foubert et al., 2008). In the light of our findings, however, they
400 could also have been negatively affected by periods of intensive seepage during higher tectonic activity. Future
401 studies are important to test this hypothesis in greater detail.

402 4.3. Spatio-temporal co-existence of CWCs and chemosynthetic organisms — the buffer effect

403 As discussed above, MDAC deposits are ecologically beneficial for CWCs, as they served as optimal substrata
404 even when seepage is still present (e. g. Hovland, 1990; Hovland & Thomsen, 1997; Le Guilloux et al., 2009; this
405 study). Severe hydrocarbon-rich seepage, however, is ecologically stressful for the corals. Particularly, fluid- and
406 AOM-derived hydrogen sulfide is considered problematic because of its role in coral necrosis (Myers &
407 Richardson, 2009; García et al., 2016) and carbonate dissolution effects (Wehrmann et al., 2011).

408 Hydrogen sulfides can efficiently be buffered through the reaction with Fe-(oxyhydro)-oxides or Fe²⁺ dissolved in
409 pore waters, ultimately forming pyrite (Wehrmann et al., 2011). Fe-(oxyhydro)-oxides nodules have previously
410 been observed in the Iberian and Moroccan margins (González et al., 2009; 2012b), but not in the Pompeia
411 Province. Instead, sulfide-oxidizing bacteria living in symbiosis with invertebrates (e.g. siboglinid worms:
412 Petersen & Dubilier, 2009) (Fig. 5, D) and thriving in mats (Fig. 4, C; Fig. 6, A) were particularly prominent along
413 this region. These microbes may form a biological buffer by withdrawing reduced sulfur species through their
414 metabolic activity. Likewise, Furthermore, the consumption of methane and sulfate by AOM-microorganisms at
415 active sites also contribute to CWCs colonization of the carbonates by reducing environmental acidification.

416 We propose that this biological buffer provides a further ecological linkage between hydrocarbon-rich seepage
417 and cold-water corals along the Pompeia Province ("buffer effect model": Fig. 12). This model explains the
418 observed co-existence of non-chemosynthetic corals (e.g. on top of D10-R7 carbonate: Fig. 5) with AOM-
419 microorganisms and chemosynthetic sulfide-oxidizing organisms at pockmark sites at the Al Gacel MV (Fig. 12,
420 A). At the same time, it is in line with associations of sulfide-oxidizing bacterial mats, scleractinian corals, and
421 other non-chemosynthetic octocorals at diapiric ridges and coral mounds in the Northern Pompeia Coral Ridge
422 (Fig. 12, B, C). The impact and exact capacity of this biological buffer, however, remains elusive and must be
423 evaluated in future studies. An integrated model is proposed to represent the biological buffer effect observed in
424 different cases along the Pompeia Province. On the one hand, pockmark sites at the Al Gacel MV display the co-

425 ~~existence of non-chemosynthetic corals (e.g. on top of D10 R7 carbonate; Fig. 5) with AOM microorganisms and~~
426 ~~chemosynthetic sulfide oxidizing organisms (Fig. 12, A). Likewise, diapiric ridges (Fig. 12, B) and coral mounds~~
427 ~~(Fig. 12, C) may similarly prevent CWCs dissolution, as observed in the Northern Pompeia Coral Ridge, where~~
428 ~~sulfide oxidizing bacterial mats were tightly related to the scleractinian coral carbonates colonized by other non-~~
429 ~~chemosynthetic octocorals (Fig. 6). This model represents the first approach on understanding the ecological~~
430 ~~linkage between hydrocarbon rich seepage and cold water corals. The impact and exact capacity of this biological~~
431 ~~buffer, however, remains elusive and must be evaluated in future studies.~~

432 **5. Conclusions**

433 The presence of cold-water corals related to hydrocarbon-seep structures like mud volcanoes and diapirs, is partly
434 due to the irregular topography affecting bottom water-currents, which supply nutrients to the corals. Likewise,
435 their tight-linkage to active hydrocarbon-rich seepage occurs by means of the production of methane-derived
436 carbonates and how they provide the hard substrata cold-water corals need to develop. The discovery of methane-
437 derived carbonates with embedded corals evidences the decline of coral colonization when the intensity of the
438 fluid seepage increases or becomes more violent. Consequently, cold-water coral growth in these habitats depends
439 directly on seepage intensity and how these fluids are drained onto the seafloor (i.e. eruptive, focused, diffused or
440 dripping-like). Furthermore, cold-water corals rely on the microbial AOM-metabolism and sulfide oxidation to
441 reduce seeped fluids in the environment, since they are harmful for the corals. This biological buffer is possibly
442 crucial to keep conditions favorable for the growth of cold-water corals in the studied area, particularly in times
443 of increased fluid seepage.

444 **Author contribution**

445 Blanca Rincón-Tomás, Dominik Schneider and Michael Hoppert carried out the microbial analysis. Jan-Peter
446 Duda carried out the biomarker analysis. Luis Somoza and Teresa Medialdea processed seismic and bathymetric
447 data. Pedro Madureira processed ROV data. Javier González and Joachim Reitner carried out the petrographic
448 analysis. Joachim Reitner carried out the stable isotopic analysis. Blanca Rincón-Tomás prepared the manuscript
449 with contributions from all co-authors.

450 **Competing interests**

451 The authors declare that they have no conflict of interest.

452 **Acknowledgments**

453 The authors thank the captain and the crew on board the R/V Sarmiento de Gamboa, as well as the UTM (Unidad
454 de Tecnología Marina), that have been essential for the success of this paper. Data obtained on board is collected
455 in the SUBVENT-2 cruise, which can be found in the IGME archive. This work was supported by the Spanish
456 project SUBVENT (CGL2012-39524-C02) and the project EXPLOSEA (CTM2016-75947) funded by the Spanish
457 Ministry of Science, Innovation and Universities.

458 **References**

- 459 Ahmed, M. and George, S.C.: Changes in the molecular composition of crude oils during their preparation for GC
 460 and GC–MS analyses, *Org. Geochem.*, 35, 137–155, doi:10.1016/j.orggeochem.2003.10.002, 2004.
- 461 Becker, E. L., Cordes, E. E., Macko, S. A., and Fisher, C. R.: Importance of seep primary production to *Lophelia*
 462 *pertusa* and associated fauna in the Gulf of Mexico, *Deep-sea Res Pt I*, 56(5), 786–800,
 463 doi:10.1016/j.dsr.2008.12.006, 2009.
- 464 Birgel, D., Thiel, V., Hinrichs, K. U., Elvert, M., Campbell, K. A., Reitner, J., Farmer, J. D., and Peckmann, J.:
 465 Lipid biomarker patterns of methane-seep microbialites from the Mesozoic convergent margin of
 466 California, *Org. Geochem.*, 37(10), 1289–1302, doi:10.1016/j.orggeochem.2006.02.004, 2006.
- 467 Boetius, A., Ravensschlag, K., Schubert, C. J., Rickert, D., Widdeh, F., Gieseke, A., Amann, R., Jørgensen, B. B.,
 468 Witte, U., and Pfannkuche, O.: A marine microbial consortium apparently mediating anaerobic oxidation
 469 of methane, *Nature*, 407 (6804), 623–626, doi:10.1038/35036572, 2000.
- 470 ~~Boetius, A., and Suess, E.: Hydrate Ridge: a natural laboratory for the study of microbial life fueled by methane
 471 from near surface gas hydrates, *Chem. Geol.*, 205, 291–310, doi:10.1016/j.chemgeo.2003.12.034, 2004.~~
- 472 Callahan, B., MacMurdie, P. J., and Holmes, S. O.: Exact sequence variants should replace optional taxonomic
 473 units in marker-gene data analysis, *ISME J.*, 11, 2639–2643, doi:10.1038/ismej.2017.119, 2017.
- 474 Caporaso, J.G., Kuczynski, J., Stombaugh, J., Bittinger, K., Bushman, F.D., Costello, E.K., Fierer, N., González-
 475 Peña, A., Goodrich, J. K., Gordon, J. I., Huttley, G. A., Knights, D., Koenig, J. E., Lozupone, C. A.,
 476 McDonald, D., Muegge, B. D., Pirrung, M., Reeder, J., Sevinsky, J. R., Turnbaugh, P. J., Walters, W. A.,
 477 Widmann, J., Yatsunenko, T., Zaneveld, J., and Knight, R.: QIIME allows analysis of high-throughput
 478 community sequencing data, *Nat. Methods*, 7, 335–336, doi:10.1038/nmeth.f.303, 2010.
- 479 Cordes, E., Arnaud-Haond, S., Bergstad, O., da Costa Falcão, A. P., Freiwald, A., Roberts, J. M., and Bernal, P.:
 480 Cold water corals, in: *The First Global Integrated Marine Assessment, World Ocean Assessment I*, United
 481 Nations, Cambridge University Press, Cambridge, United Kingdom, 2016.
- 482 Díaz-del-Río, V., Somoza, L., Martínez-Frías, J., Mata, M. P., Delgado, A., Hernandez-Molina, F. J., ..., Vázquez,
 483 J. T.: Vast fields of hydrocarbon-derived carbonate chimneys related to the accretionary
 484 wedge/olistostrome of the Gulf of Cádiz, *Mar. Geol.*, 195, 177–200, doi:10.1016/S0025-3227(02)00687-
 485 4, 2003.
- 486 Dorschel, B., Hebbeln, D., Foubert, A., White, M., and Wheeler, A. J.: Hydrodynamics and cold-water coral facies
 487 distribution related to recent sedimentary processes at Galway Mound west of Ireland, *Mar. Geol.*, 244,
 488 184–195, doi:10.1016/j.margeo.2007.06.010, 2007.
- 489 Duineveld, G. C., Lavaleye, M. S., Bergman, M. J., De Stigter, H., and Mienis, F.: Trophic structure of a cold-
 490 water coral mound community (Rockall Bank, NE Atlantic) in relation to the near-bottom particle supply
 491 and current regime, *B. Mar. Sci.*, 81 (3), 449–467, 2007.
- 492 Dullo, W. C., Flügel, S., and Rüggerberg, A.: Cold-water coral growth in relation to the hydrography of the Celtic
 493 and Nordic European continental margin, *Mar. Ecol. Prog. Ser.*, 371, 165–176, doi:10.3354/meps07623,
 494 2008.
- 495 Dunham, R. J., 1962, Classification of carbonate rocks according to their depositional texture, in: *Classification*
 496 *of Carbonate Rocks*, Ham, W. E. (Eds.), American Association of Petroleum Geologists Memoir 1, Tulsa,
 497 OK, 108–121, 1962.
- 498 Edgar, R. C.: USEARCH. <http://www.drive5.com/usearch>. 2010.

499 Egelkamp, R., Schneider, D., Hertel, R., and Daniel, R.: Nitrile-Degrading Bacteria Isolated from Compost, *Front.*
500 *Environ. Sci.*, 5, doi: 10.3389/fenvs.2017.00056, 2017.

501 Embry III, A. F., and Klovan, J. E.: A late Devonian reef tract on northeastern Banks Island, NWT, B. *Can. Petrol.*
502 *Geol.*, 19(4), 730–781, 1971.

503 Foubert, A., Depreiter, D., Beck, T., Maignien, L., Pannemans, B., Frank, N., Blamart, D., and Henriët, J.:
504 Carbonate mounds in a mud volcano province off north-west Morocco: key to processes and controls,
505 *Mar. Geol.*, 248, 74–96, doi: 10.1016/j.margeo.2007.10.012, 2008.

506 ~~Frank, N., Freiwald, A., López-Correa, M., Wienberg, C., Eisele, M., Hebbeln, D., Van Rooij, D., Henriët, J. P.,~~
507 ~~Colin, C., van Weering, T., de Haas, H., Buhl-Mortensen, P., Roberts, J. M., De Mol, B., Douville, E.,~~
508 ~~Blamart, D., and Hatté, C.: Northeastern Atlantic cold-water coral reefs and climate, *Geology*, 39 (8),~~
509 ~~743–746, doi:10.1130/G31825.1, 2011.~~

510 ~~Freiwald, A., Hühnerbach, V., Lindberg, B., Wilson, J., and Campbell, J.: The Sula Reef Complex, Norwegian~~
511 ~~Shelf, *Facies*, 47, 179–200, doi:10.1007/BF02667712, 2002.~~

512 ~~Freiwald, A., Wilson, J. B., and Henrich, R.: Grounding Pleistocene icebergs shape recent deep-water coral reefs,~~
513 ~~*Sedimentary Geology* 125, 1–8, doi:10.1016/S0037-0738(98)00142-0, 1999.~~

514 Garcia, G. D., Santos, E. D. O., Sousa, G. V., Zingali, R. B., Thompson, C. C., and Thompson, F. L.:
515 Metaproteomics reveals metabolic transitions between healthy and diseased stony coral *Mussismilia*
516 *braziliensis*, *Mol. Ecol.*, 25(18), 4632–4644, doi:10.1111/mec.13775, 2016.

517 ~~Goedert, J. L., and Peckmann, J.: Corals from deep-water methane-seep deposits in Paleogene strata of Western~~
518 ~~Oregon and Washington, U.S.A., in: *Cold-water corals and Ecosystems*, Freiwald, A., and Roberts, J. M.~~
519 ~~(eds.), Springer-Verlag, Berlin Heidelberg, 27–40, 2005.~~

520 Gomes-Sumida, P. Y., Yoshinaga, M. Y., Saint-Pastous Madureira, L. A., and Hovland, M.: Seabed pockmarks
521 associated with deep water corals off SE Brazilian continental slope, Santos Basin, *Mar. Geol.*, 207, 159–
522 167, doi:10.1016/j.margeo.2004.03.006, 2004.

523 González, F. J., Somoza, L., Lunar, R., Martínez-Frías, J., Martín Rubí, J. A., Torres, T., Ortiz, J. E., Díaz-del-
524 Río, V., Pinheiro, L. M., and Magalhães, V. H.: Hydrocarbon-derived ferromanganese nodules in
525 carbonate mud mounds from the Gulf of Cádiz: mud-breccia sediments and clasts as nucleation sites,
526 *Mar. Geol.*, 261, 64–81, doi:10.1016/j.margeo.2008.11.005, 2009.

527 González, F. J., Somoza, L., León, R., Medialdea, T., de Torres, T., Ortiz, J. E., Martínez-Frías, J., and Merinero,
528 R.: Ferromanganese nodules and micro-hardgrounds associated with the Cádiz Contourite Channel (NE
529 Atlantic): Palaeoenvironmental records of fluid venting and bottom currents, *Chem. Geol.*, 310–311, 56–
530 78, doi: 10.1016/j.chemgeo.2012.03.030, 2012a.

531 González, F. J., Somoza, L., Medialdea, T., León, R., Torres, T., Ortiz, J. E., and Martín-Rubí, J. A.: Discovery of
532 ferromanganese hydrocarbon-related nodules associated with the Meknes mud volcano (Western
533 Moroccan margin). European Geoscience Union 2012 (EGU2012). Viena (Austria). *Geophys. Res. Abs.*
534 vol. 14, EGU2012-12306, 2012b.

535 Hebbeln, D., Van Rooij, D., and Wienberg, C.: Good neighbours shaped by vigorous currents: cold-water coral
536 mounds and contourites in the North Atlantic, *Mar. Geol.*, 378, 171–185,
537 doi:10.1016/j.margeo.2016.01.014, 2016.

538 Hensen, C., Nuzzo, M., Hornibrook, E., Pinheiro, L.M., Bock, B., Magalhães, V.H., and Brückmann, W.: Sources
539 of mud volcano fluids in the Gulf of Cádiz — indications for hydrothermal imprint, *Geochim.*
540 *Cosmochim. Ac.*, 71 (5), 1232–1248, doi:10.1016/j.gca.2006.11.022, 2007.

541 Hinrichs, K. -U., and Boetius, A.: The anaerobic oxidation of methane: new insights in microbial ecology and
542 biogeochemistry, in: *Ocean Margin Systems*, Wefer, G., Billett, D., Hebbeln, D., Jørgensen, B.B.,
543 Schlueter, M., Van Weering, T. (Eds.), Springer-Verlag, Berlin, 457–477, 2002.

544 Hinrichs, K. -U., Hayes, J. M., Sylva, S. P., Brewer, P. G., and De Long, E. F.: Methane-consuming archaeobacteria
545 in marine sediments, *Nature*, 398, 802–805, doi:10.1038/19751, 1999.

546 Hoefs, J.: *Stable Isotope Geochemistry*, Springer, Berlin, 2015.

547 Hovland, M.: Do carbonate reefs form due to fluid seepage?, *Terra Nova*, 2, 8–18, doi:10.1111/j.1365-
548 3121.1990.tb00031.x, 1990.

549 Hovland, M., Jensen, S., and Indreien, T.: Unit pockmarks associated with *Lophelia* coral reefs off mid-Norway:
550 more evidence of control by ‘fertilizing’ bottom currents, *Geo-Mar. Lett.*, 32 (5–6), 545–554,
551 doi:10.1007/s00367-012-0284-0, 2012.

552 Hovland, M., Mortensen, P. B., Brattegard, T., Strass, P., and Rokoengen, K.: Ahermatypic coral banks off mid-
553 Norway: evidence for a link with seepage of light hydrocarbons, *Palaios*, 13, 189–200, doi:10.1043/0883-
554 1351(1998)013<0189:ACBOME>2.0.CO;2, 1998.

555 Hovland, M., and Thomsen, E.: Cold-water corals — are they hydrocarbon seep related?, *Mar. Geol.*, 137, 159–
556 164, doi:10.1016/S0025-3227(96)00086-2, 1997.

557 Huvenne, V. A., Masson, D. G., and Wheeler, A. J.: Sediment dynamics of a sandy contourite: the sedimentary
558 context of the Darwin cold-water coral mounds, Northern Rockall Trough, *Int. J. Earth Sci.*, 98 (4), 865–
559 884, doi: 10.1007/s00531-008-0312-5, 2009.

560 Ivanov, M. K., Akhmetzhanov, A. M., and Akhmanov, G. G.: Multidisciplinary study of geological processes on
561 the North East Atlantic and Western Mediterranean Margins, in: *Ioc. Tech. S.*, 56, UNESCO, 2000.

562 Kiriakoulakis, K., Fisher, E., Wolff, G. A., Freiwald, A., Grehan, A., and Roberts, J. M.: Lipids and nitrogen
563 isotopes of two deep-water corals from the North-East Atlantic: initial results and implications for their
564 nutrition, in: *Cold-Water Corals and Ecosystems*, Freiwald, A., Roberts, J. M. (Eds.), Erlangen Earth
565 Conf., Springer, Germany, 715–729, 2005.

566 Le Bris, N., Arnaud-Haond, S., Beaulieu, S., Cordes, E. E., Hilario, A., Rogers, A., van de Gaever, S., and
567 Watanabe, H.: Hydrothermal Vents and Cold Seeps, in: *The First Global Integrated Marine Assessment*,
568 United Nations, Cambridge University Press, Cambridge, United Kingdom, 2016.

569 Le Guilloux, E., Olu, K., Bourillet, J. F., Savoye, B., Iglésias, S. P., and Sibuet, M.: First observations of deep-sea
570 coral reefs along the Angola margin, *Deep-sea Res. Pt. II*, 56, 2394–2403,
571 doi:10.1016/j.dsr2.2009.04.014, 2009.

572 Liebetrau, V., Eisenhauer, A., and Linke, P.: Cold seep carbonates and associated cold-water corals at the
573 Hikurangi Margin, New Zealand: new insights into fluid pathways, growth structures and geochronology,
574 *Mar. Geol.*, 272, 307–318, doi:10.1016/j.margeo.2010.01.003, 2010.

575 León, R., Somoza, L., Medialdea, T., Vázquez, J. T., González, F. J., López-González, N., Casas, D., del Pilar
576 Mata, M., del Fernández-Puga, C., Giménez-Moreno, C. J., and Díaz-del-Río, V.: New discoveries of
577 mud volcanoes on the Moroccan Atlantic continental margin (Gulf of Cádiz): morpho-structural
578 characterization, *Geo-Mar. Lett.*, 32, 473–488, doi:10.1007/s00367-012-0275-1, 2012.

579 Magalhães, V. H., Pinheiro, L. M., Ivanov, M. K., Kozlova, E., Blinova, V., Kolganova, J., Vasconcelos, C.,
580 McKenzie, J. A., Bernasconi, S. M., Kopf, A., Díaz-del-Río, V., González, F. J., and Somoza, L.:
581 Formation processes of methane-derived authigenic carbonates from the Gulf of Cádiz, *Sediment. Geol.*,
582 243–244, 155–168, doi:10.1016/j.sedgeo.2011.10.013, 2012.

583 Margreth, S., Gennari, G., Rüggeberg, A., Comas, M. C., Pinheiro, L. M., and Spezzferri, S.: Growth and demise
584 of cold-water coral ecosystems on mud volcanoes in the West Alboran Sea: The messages from planktonic
585 and benthic foraminifera, *Mar. Geol.*, 282, 26–39, doi:10.1016/j.margeo.2011.02.006, 2011.

586 Martin, M.: Cutadapt removes Adapter Sequences from High-Throughput Sequencing Reads, *EMBnet.journal*, 10–
587 12, doi: 10.14806/ej.17.1.200, 2011.

588 Medialdea, T., Somoza, L., Pinheiro, L. M., Fernández-Puga, M. C., Vázquez, J. T., León, R., Ivanov, M. K.,
589 Magalhães, V., Díaz-del-Río, V., and Vegas, R.: Tectonics and mud volcano development in the Gulf of
590 Cádiz, *Mar. Geol.*, 261, 48–63, doi:10.1016/j.margeo.2008.10.007, 2009.

591 Mortensen, P. B., Hovland, M. T., Fossa, J. H., and Furevik, D. M.: Distribution, abundance and size of *Lophelia*
592 *pertusa* coral reefs in mid Norway in relation to seabed characteristics, *J. Mar. Biol. Assoc. UK*, 81, 581–
593 597, doi:10.1017/S002531540100426X, 2001.

594 Myers, J.L., and Richardson, L.L.: Adaptation of cyanobacteria to the sulfide-rich microenvironment of black band
595 disease of coral, *FEMS Microbiol. Ecol.*, 67, 242–251, doi:10.1111/j.1574-6941.2008.00619.x, 2009.

596 Peckmann, J., Reimer, A., Luth, U., Luth, C., Hansen, B.T., Heinicke, C., Hoefs, J., and Reitner, J.: Methane-
597 derived carbonates and authigenic pyrite from the northwestern Black Sea, *Mar. Geol.*, 177, 129–150,
598 doi:10.1016/S0025-3227(01)00128-1, 2001.

599 Peckmann, J., and Thiel, V.: Carbon cycling at ancient methane-seeps, *Chem. Geol.*, 205 (3), 443–467,
600 doi:10.1016/j.chemgeo.2003.12.025, 2004.

601 Petersen, J. M., and Dubilier, N.: Methanotrophic symbioses in marine invertebrates, *Env. Microbiol. Rep.*, 1(5),
602 319–335, doi:10.1111/j.1758-2229.2009.00081.x, 2009.

603 Pinheiro, L. M., Ivanov, M. K., Sautkin, A., Akhmanov, G., Magalhães, V. H., Volkonskaya, A., Monteiro, J. H.,
604 Somoza, L., Gardner, J., Hamouni, N., and Cunha, M. R.: Mud volcanism in the Gulf of Cádiz: results
605 from the TTR-10 cruise, *Mar. Geol.*, 195, 131–151, doi:10.1016/S0025-3227(02)00685-0, 2003.

606 Rådecker, N., Pogoreutz, C., Voolstra, C. R., Wiedenmann, J., and Wild, C.: Nitrogen cycling in corals: The key
607 to understanding holobiont functioning?, *Trends Microbiol.*, 23 (8), 490–497,
608 doi:10.1016/j.tim.2015.03.008, 2015.

609 Reitner, J., Gauret, P., Marin, F., and Neuweiler, F.: Automicrites in a modern marine microbialite. Formation
610 model via organic matrices (Lizard Island, Great Barrier Reef, Australia), *Bull.-Inst. Oceanogr. Monaco*,
611 14, 237–263, 1995.

612 Reitner, J., Peckmann, J., Blumenberg, M., Michaelis, W., Reimer, A., and Thiel, V.: Concretionary methane-seep
613 carbonates and associated microbial communities in Black Sea sediments, *Palaeogeogr., Palaeoclimatol.,*
614 *Palaeocl.*, 227, 18–30, doi:10.1016/j.palaeo.2005.04.033, 2005.

615 Roberts, J. M., Long, D., Wilson, J. B., Mortensen, P. B., and Gage, J. D.: The cold-water coral *Lophelia pertusa*
616 (Scleractinia) and enigmatic seabed mounds along the north-east Atlantic margin: are they related?, *Mar.*
617 *Pollut. Bull.*, 46, 7–20, doi:10.1016/S0025-326X(02)00259-X, 2003.

618 Roberts, J. M., Wheeler, A. J., and Freiwald, A.: Reefs of the deep: the biology and geology of cold-water coral
619 ecosystems, *Science*, 312 (5773), 543–547, doi:10.1126/science.1119861, 2006.

620 Roberts, J. M., Wheeler, A., Freiwald, A., and Cairns, S. (Eds.): Cold-water corals: the biology and geology of
621 deep-sea coral habitats, Cambridge University Press, Cambridge, United Kingdom, 2009.

622 Rodrigues, C. F., Cunha, M. R., Génio, L., and Duperron, S.: A complex picture of associations between two host
623 mussels and symbiotic bacteria in the Northeast Atlantic, *Naturwissenschaften*, 100, 21–31,
624 doi:10.1007/s00114-012-0985-2, 2013.

625 Rogers, A. D.: The Biology of *Lophelia pertusa* (Linnaeus 1758) and other Deep-Water Reef-Forming Corals and
626 Impacts from Human Activities, *Int. Rev. Hydrobiol.*, 84 (4), 315–406, doi:10.1002/iroh.199900032,
627 1999.

628 Rueda, J. L., González-García, E., Krutzky, C., López-Rodríguez, J., Bruque, G., López-González, N., Palomino,
629 D., Sánchez, R. F., Vázquez, J. T., Fernández-Salas, L. M., and Díaz-del-Río, V.: From chemosynthetic-
630 based communities to cold-water corals: Vulnerable deep-sea habitats of the Gulf of Cádiz, *Mar.*
631 *Biodiver.*, 46, 473–482, doi:10.1007/s12526-015-0366-0, 2016.

632 Sánchez-Guillamón, O., García, M. C., Moya-Ruiz, F., Vázquez, J. T., Palomino, D., Fernández-Puga, M. C., and
633 Sierra, A.: A preliminary characterization of greenhouse gas (CH₄ and CO₂) emissions from Gulf of Cádiz
634 mud volcanoes, VIII Symposium MIA15, 2015.

635 ~~Scholz, F., Hensen, C., Reitz, A., Romer, R. L., Liebetrau, V., Meixner, A., Weise, S. M., and Haeckel, M.: Isotopic
636 evidence (⁸⁷Sr/⁸⁶Sr, ⁸⁷Li) for alteration of the oceanic crust at deep-rooted mud volcanoes in the Gulf
637 of Cádiz, NE Atlantic Ocean, *Geochim. Cosmochim. Ac.*, 73, 5444–5459, doi:10.1016/j.gea.2009.06.004,
638 2009.~~

639 ~~Smith, P., Reay, D., and Van Amstel, A. (Eds.): Methane and climate change, Earthscan, London, Washington
640 D.C., 2010.~~

641 Somoza, L., Ercilla, G., Ugorri, V., León, R., Medialdea, T., Paredes, M., González, F. J., and Nombela, M. A.:
642 Detection and mapping of cold-water coral mounds and living *Lophelia* reefs in the Galicia Bank, Atlantic
643 NW Iberia margin, *Mar. Geol.*, 349, 73–90, doi:10.1016/j.margeo.2013.12.017, 2014.

644 Somoza, L., León, R., Ivanov, M. Fernández-Puga, M. C., Gardner, J. M., Hernández-Molina, F. J., Pinheiro, L.
645 M., Rodero, J., Lobato, A., Maestro, A., Vázquez, J. T., Medialdea, T., and Fernández-Salas, L. M.:
646 Seabed morphology and hydrocarbon seepage in the Gulf of Cádiz mud volcano area: Acoustic imagery,
647 multibeam and ultra-high resolution seismic data, *Mar. Geol.*, 195, 153–176, doi:10.1016/S0025-
648 3227(02)00686-2, 2003.

649 Sorokin, Y. I.: Coral reef ecology, Springer, Germany, 1995.

650 Suess, E., and Whiticar, M. J.: Methane-derived CO₂ in pore fluids expelled from the Oregon subduction zone,
651 *Palaeogeogr., Palaeoclimatol., Palaeocl.*, 71, 119–136, doi:10.1016/0031-0182(89)90033-3, 1989.

652 Thiel, V., Peckmann, J., Seifert, R., Wehrung, P., Reitner, J., and Michaelis, W.: Highly isotopically depleted
653 isoprenoids: molecular markers for ancient methane venting, *Geochim. Cosmochim. Ac.*, 63, 3959–3966,
654 doi:10.1016/S0016-7037(99)00177-5, 1999.

655 Thiel, V., Peckmann, J., Richnow, H.-H., Luth, U., Reitner, J., and Michaelis, W.: Molecular signals for anaerobic
656 methane oxidation in Black Sea seep carbonates and a microbial mat, *Mar. Chem.* 73, 97–112,
657 doi:10.1016/S0304-4203(00)00099-2, 2001.

658 Thiem, Ø., Ravagnan, E., Fosså, J. H., and Berntsen, J.: Food supply mechanisms for cold- water corals along a
659 continental shelf edge, *J. Marine Syst.*, 26, 1481–1495, doi:10.1016/j.jmarsys.2005.12.004, 2006.

Código de campo cambiado

660 [Valentine, D. L.: Biogeochemistry and microbial ecology of methane oxidation in anoxic environments: a review,](#)
661 [A. Van Leeuw. J. Microb., 81, 271–282, doi:10.1023/A:1020587206351, 2002.](#)

662 Vandorpe, T., Martins, I., Vitorino, J., Hebbeln, D., García-García, M., and Van Rooij, D.: Bottom currents and
663 their influence on the sedimentation pattern in the El Arraiche mud volcano province, southern Gulf of
664 Cádiz, *Mar. Geol.*, 378, 114–126, doi:10.1016/j.margeo.2015.11.012, 2016.

665 Vandorpe, T., Wienberg, C., Hebbeln, D., Van den Berghe, M., Gaide, S., Wintersteller, P., and Van Rooij, D.:
666 Multiple generations of buried cold-water coral mounds since the Early-Middle Pleistocene Transition in
667 the Atlantic Moroccan Coral Province, southern Gulf of Cádiz, *Palaeogeogr., Palaeoclimatol., Palaeocl.*,
668 485, 293–304, doi:10.1016/j.palaeo.2017.06.021, 2017.

669 Van Rensbergen, P., Depreiter, D., Pannemans, B., Moerkerke, G., Van Rooij, D., Marsset, B., Akhmanov, G.,
670 Blinova, V., Ivanov, M., Rachidi, M., Magalhães, V., Pinheiro, L., Cunha, M., and Henriët, J.P.: The
671 Arraiche mud volcano field at the Moroccan Atlantic slope, Gulf of Cádiz, *Mar. Geol.*, 219, 1–17,
672 doi:10.1016/j.margeo.2005.04.007, 2005.

673 Van Rooij, D., Blamart, D., De Mol, L., Mienis, F., Pirlet, H., Whermann, L. M., ..., Henriët, J. -P.: Cold-water
674 coral mounds on the Pen Duick Escarpment, Gulf of Cádiz: The MiCROSYSTEMS project approach,
675 *Mar. Geol.*, 282, 102–117, doi:10.1016/j.margeo.2010.08.012, 2011.

676 Watling, L., France, S. C., Pante, E., and Simpson, A.: Biology of Deep-Water Octocorals, in: *Advances in Marine*
677 *Biology Volume 60*, Lesser, M. (Eds.), Academic Press, London, United Kingdom, 41–122, 2011.

678 Webster, N. S., Negri, A. P., Botté, E. S., Laffy, P. W., Flores, F., Noonan, S., Schmidt, C., and Uthicke, S.: Host-
679 associated coral reef microbes respond to the cumulative pressures of ocean warming and ocean
680 acidification *Sci. Rep.-UK*, 6, doi:10.1038/srep19324, 2016.

681 Wheeler, A. J., Beyer, A., Freiwald, A., de Haas, H., Huvenne, V. A., Kozachenko, M., Olu-Le Roy, K.,
682 and Opderbecke, J.: Morphology and environment of cold-water coral carbonate mounds on the NW
683 European margin, *Int. J. Earth Sci.*, 96, 37–56, doi:10.1007/s00531-006-0130-6, 2007.

684 Wehrmann, L. M. Templer, S. P., Brunner, B., Bernasconi, S. M., Maignien, L., and Ferdelman, T. G.: The imprint
685 of methane seepage on the geochemical record an early diagenetic processes in cold-water coral mounds
686 on Pen Duick Escarpment, Gulf of Cádiz, *Mar. Geol.*, 118–137, doi:10.1016/j.margeo.2010.08.005, 2011.

687 Wienberg, C., Hebbeln, D., Fink, H. G., Mienis, F., Dorschel, B., Vertino, A., López-Correa, M., and Freiwald,
688 A.: Scleractinian cold-water corals in the Gulf of Cádiz—first clues about their spatial and temporal
689 distribution, *Deep-sea Res. Pt. I*, 56 (10), 1873–1893, doi:10.1016/j.dsr.2009.05.016, 2009.

690 Wienberg, C., and Titschack, J.: Framework-forming scleractinian cold-water corals through space and time: a
691 late Quaternary North Atlantic perspective, in: *Marine Animal Forests: The Ecology of Benthic*
692 *Biodiversity Hotspots*, Rossi, S., Bramanti, L., Gori, A., and Orejas, C. (Eds.), Springer, Cham,
693 Switzerland, 1–34, 2015.

694 Yilmaz, P., Parfrey, L.W., Yarza, P., Gerken, J., Pruese, E., Quast, C., Schweer, T., Peplies, J., Ludwig, W., and
695 Glöckner, F. O.: The SILVA and ‘All-species Living Tree Project (LTP)’ taxonomic frameworks, *Nucleic*
696 *Acids Res.*, 42, D643–D648, doi:10.1093/nar/gkt1209, 2014.

697 Zhang, J., Kobert, K., Flouri, T., and Stamatakis, A.: PEAR: a fast and accurate Illumina Paired-End reAd
698 merger, *Bioinformatics*, 30 (5), 614–620, doi:10.1093/bioinformatics/btt593, 2014.

699
700

701
702
703
704
705
706
707
708
709
710
711
712
713
714
715
716
717
718
719
720
721
722
723
724
725
726
727
728
729
730
731
732
733
734
735

Table 1. *In-situ* water variables measured during sampling with ROV sensors.

	D10-R3	D10-R7	D11-R8	D03-B1
Temperature (°C)	10.07	10.5	10.02	10.04 – 10.05
Depth (m)	850 – 890	791	763	829
Conductivity (mS/cm)	39.13 – 39.62	39.05 – 39.43	-	-

Salinity (ppt)	-	-	35.56 – 35.86	35.67 – 35.91
Saturation of dissolved oxygen (%)	53.64 – 54.69	54.02 – 54.35	51.95 – 53.92	52.46 – 56.22
Dissolved oxygen (mg/l)	4.81 – 4.90	4.85 – 4.88	4.66 – 4.84	4.71 – 5.09
Density (kg/m ³)	31.03 – 31.42	30.94 – 31.24	30.92 – 31.08	31.26 – 31.41

736
737
738
739
740
741
742
743
744
745
746
747
748
749
750
751
752
753
754
755
756
757
758
759
760
761
762
763

Table 2. Stable carbon and oxygen isotopes ($\delta^{13}\text{C}$, $\delta^{18}\text{O}$) of samples from the Al Gacel MV and the Northern Pompeia Coral Ridge.

<u>Location</u>	<u>Sample</u>	<u>Origin of the carbonate</u>	<u>Identification number in Fig. 7</u>	<u>$\delta^{18}\text{O}$ (‰)</u>	<u>$\delta^{13}\text{C}$ (‰)</u>
Al Gacel MV	D10-R3	Coral skeleton	1	2.35	-5.58
			2	3.37	-20.07

		<u>Authigenic carbonate</u>	<u>3</u>	<u>3.60</u>	<u>-26.68</u>		
			<u>4</u>	<u>3.70</u>	<u>-20.79</u>		
			<u>5</u>	<u>3.45</u>	<u>-22.43</u>		
					<u>6</u>	<u>3.80</u>	<u>-20.70</u>
		<u>Coral skeleton</u>	<u>7</u>	<u>3.28</u>	<u>-2.23</u>		
			<u>8</u>	<u>3.83</u>	<u>-25.16</u>		
			<u>9</u>	<u>3.63</u>	<u>-25.29</u>		
		<u>Authigenic carbonate</u>	<u>10</u>	<u>3.91</u>	<u>-18.38</u>		
			<u>11</u>	<u>3.60</u>	<u>-24.18</u>		
			<u>12</u>	<u>3.55</u>	<u>-25.34</u>		
			<u>13</u>	<u>3.56</u>	<u>-25.15</u>		
		<u>Coral skeleton</u>	<u>14</u>	<u>3.50</u>	<u>-2.09</u>		
		<u>Authigenic carbonate</u>	<u>15</u>	<u>3.92</u>	<u>-21.89</u>		
		<u>D10-R7</u>	<u>Authigenic carbonate</u>	<u>21</u>	<u>2.90</u>	<u>-26.36</u>	
				<u>22</u>	<u>3.15</u>	<u>-28.77</u>	
	<u>23</u>			<u>2.94</u>	<u>-22.91</u>		
	<u>24</u>			<u>2.67</u>	<u>-21.13</u>		
	<u>25</u>			<u>2.37</u>	<u>-24.70</u>		
	<u>26</u>			<u>2.56</u>	<u>-23.60</u>		
	<u>D11-R8</u>	<u>Coral skeleton</u>	<u>16</u>	<u>1.49</u>	<u>-4.91</u>		
<u>17</u>			<u>2.13</u>	<u>-2.99</u>			
<u>Authigenic carbonate</u>		<u>18</u>	<u>1.74</u>	<u>-4.22</u>			
		<u>19</u>	<u>5.60</u>	<u>-14.82</u>			
		<u>20</u>	<u>5.55</u>	<u>-14.74</u>			
<u>Northern Pompeia Coral Ridge</u>	<u>D03-B1</u>	<u>Coral skeleton</u>	<u>1.1</u>	<u>-0.38</u>	<u>-7.93</u>		
			<u>1.2</u>	<u>-0.86</u>	<u>-7.77</u>		
			<u>1.3</u>	<u>-0.51</u>	<u>-7.35</u>		
			<u>1.5</u>	<u>1.15</u>	<u>-5.26</u>		
			<u>1.4</u>	<u>-1.03</u>	<u>-8.08</u>		
			<u>1.6</u>	<u>0.69</u>	<u>-5.96</u>		
			<u>1.7</u>	<u>0.54</u>	<u>-6.42</u>		
Location	Sample	Identifier	$\delta^{18}O$ (‰)	$\delta^{13}C$ (‰)			
<u>AlGaet-MV</u>	<u>D10-R3</u>	<u>1</u>	<u>2.35</u>	<u>-5.58</u>			
		<u>2</u>	<u>3.37</u>	<u>-20.07</u>			
		<u>3</u>	<u>3.60</u>	<u>-26.68</u>			
		<u>4</u>	<u>3.70</u>	<u>-20.79</u>			
		<u>5</u>	<u>3.45</u>	<u>-22.43</u>			

Tabla con formato

		6	3.80	-20.70	
		7	3.28	-2.23	
		8	3.83	-25.16	
		9	3.63	-25.29	
		10	3.91	-18.38	
		11	3.60	-24.18	
		12	3.55	-25.34	
		13	3.56	-25.15	
		14	3.50	-2.09	
		15	3.92	-21.89	
		D10-R7	21	2.90	-26.36
			22	3.15	-28.77
			23	2.94	-22.91
			24	2.67	-21.13
			25	2.37	-24.70
26	2.56		-23.60		
D11-R8	16	1.49	-4.91		
	17	2.13	-2.99		
	18	1.74	-4.22		
	19	5.60	-14.82		
	20	5.55	-14.74		
Conat-Ridge	D03-B1	11	-0.38	-7.93	
		12	-0.86	-7.77	
		13	-0.51	-7.35	
		15	1.15	-5.26	
		14	-1.03	-8.08	
		16	0.69	-5.96	
		17	0.54	-6.42	

764

765

766

767

Table 2. Continued

Location	Sample	Identifier	$\delta^{18}\text{O}$ (‰)	$\delta^{13}\text{C}$ (‰)
Conat-Ridge	D03-B1	3.1	1.59	-2.08
		3.2	-0.31	-6.27
		3.3	-0.89	-6.78

		3.4	-0.94	-6.73	
		3.5	1.84	-2.21	
		3.6	2.26	-1.39	
		3.7	1.74	-2.87	
<u>Location</u>	<u>Sample</u>	<u>Origin of the carbonate</u>	<u>Identification number in Fig. 7</u>	<u>$\delta^{18}\text{O}$ (‰)</u>	<u>$\delta^{13}\text{C}$ (‰)</u>
Northern Pompeia Coral Ridge	D03-B1	Coral skeleton	3.1	1.59	-2.08
			3.2	-0.31	-6.27
			3.3	-0.89	-6.78
			3.4	-0.94	-6.73
			3.5	1.84	-2.21
			3.6	2.26	-1.39
			3.7	1.74	-2.87

768

769

770 **Table 3.** Stable carbon isotopic composition ($\delta^{13}\text{C}$) of selected lipid biomarkers (in **Figure 10**). (*) Please note
771 that crocetane in D11-R8 coelutes with phytane. n.d. = not detected.

Compound	D10-R7 (‰)	D11-R8 (‰)
<i>n</i> -C ₁₇	n.d.	-33.0
<i>n</i> -C ₁₈	n.d.	-31.8
<i>n</i> -C ₁₉	n.d.	-31.1
<i>n</i> -C ₂₀	n.d.	-30.8
<i>n</i> -C ₂₁	n.d.	-31.5
<i>n</i> -C ₂₂	n.d.	-31.7
Crocetane*	-101.2	-57.2
PMI	-102.9	-74.3

772

773

774

775

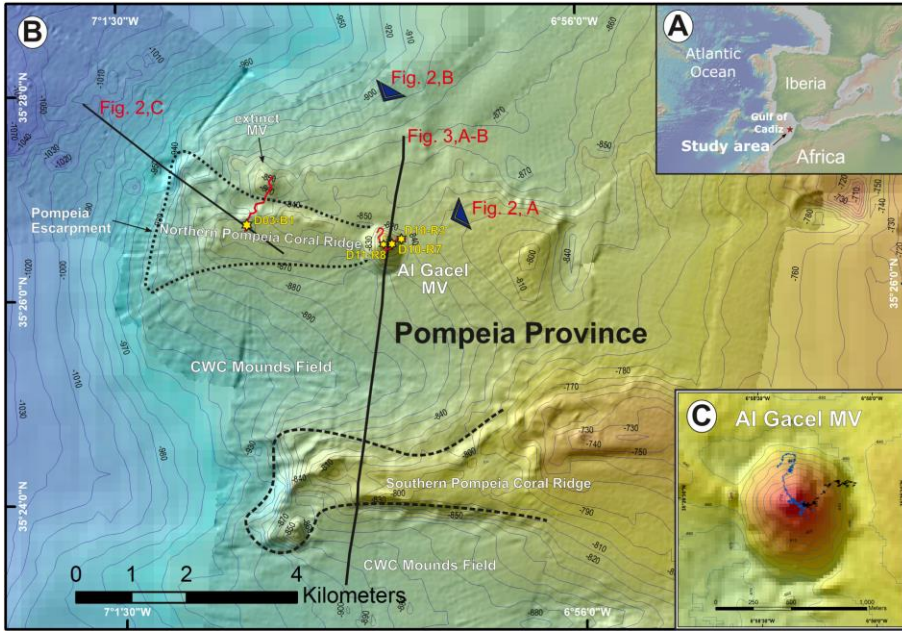
776

777

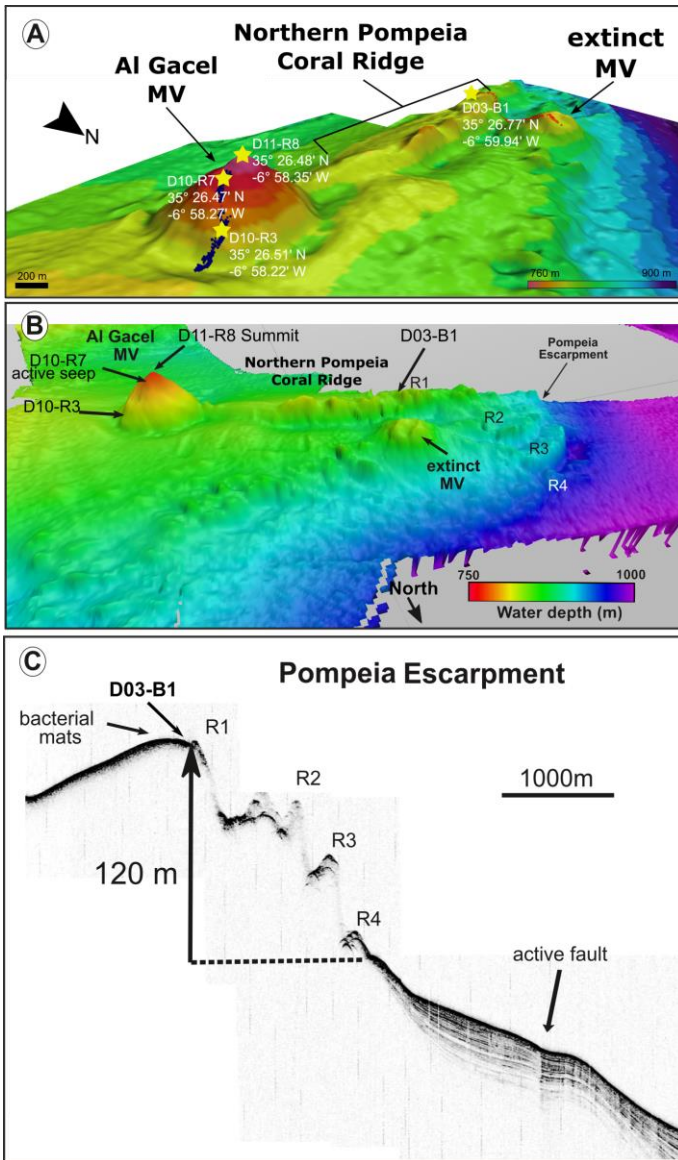
778

779

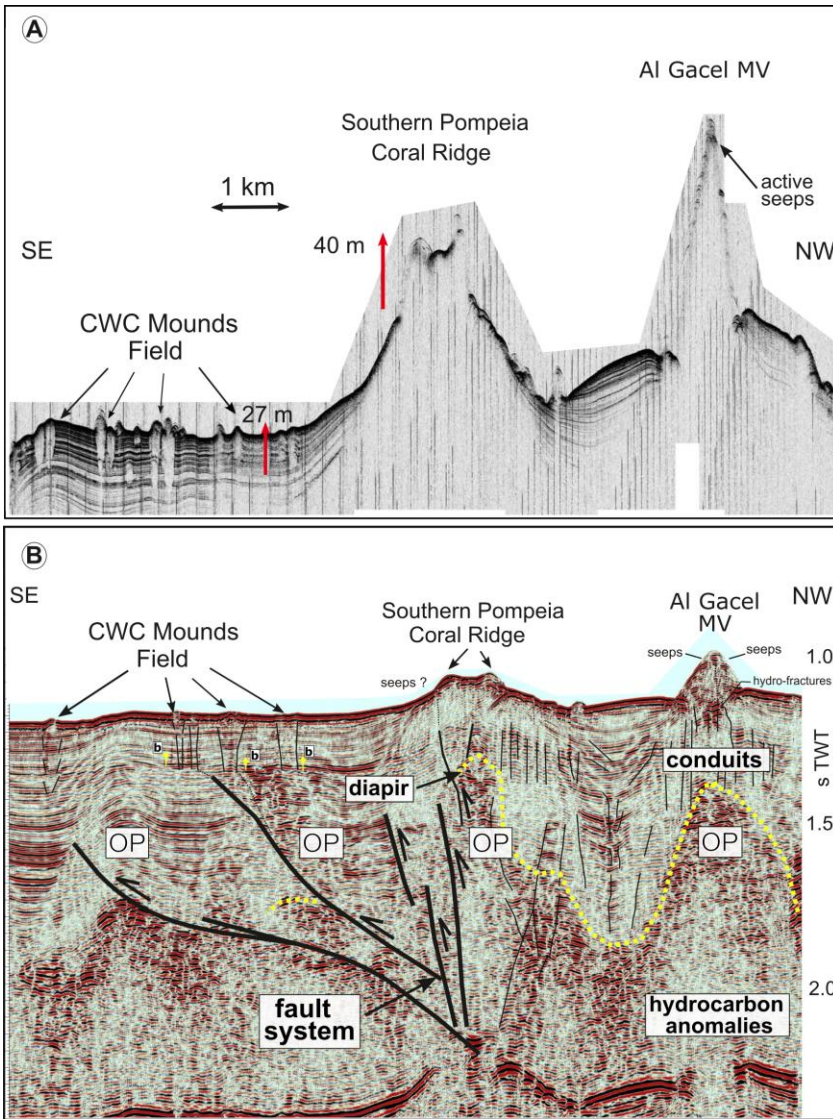
780



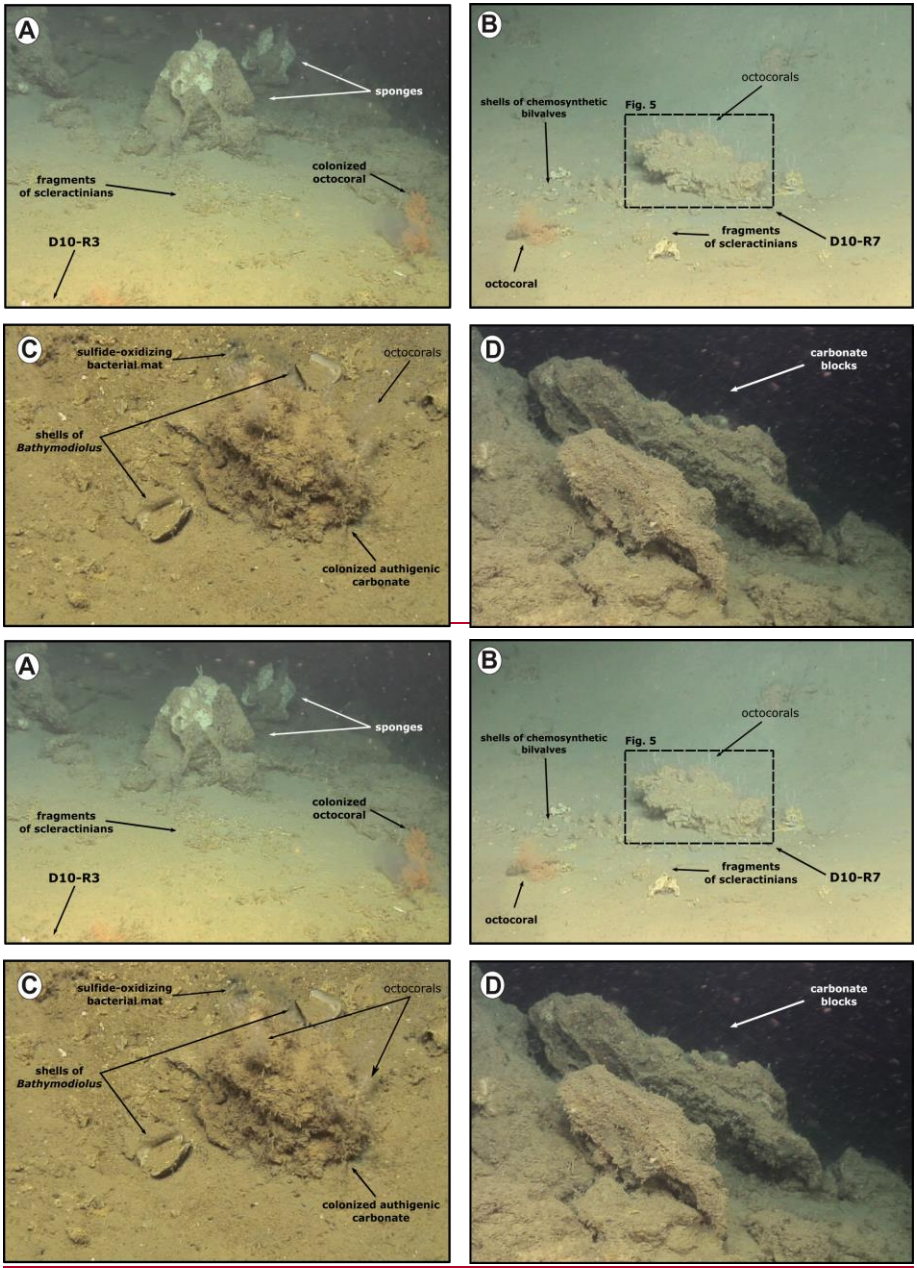
781
 782 **Figure 1.** Bathymetric map of the study area. **A:** location of the Gulf of Cádiz between Spain, Portugal and
 783 Morocco. The study area is marked with a red star; **B:** the Pompeia Province including its different morphological
 784 features. Red lines indicate ROV-paths, yellow stars mark sampling sites; **C:** detailed map of the Al Gacel MV
 785 including pathways of Dive 10 and 11 (black and blue lines, respectively). Further details of the area are provided
 786 in **Figs. 2** and **3**.



787
 788 **Figure 2.** Bathymetric and seismic maps showing morphological features in ~~the~~ northern Pompeia Province. **A–**
 789 **B:** bathymetric maps showing the Al Gacel MV, the Northern Pompeia Coral Ridge and the extinct MV. Yellow
 790 stars mark sampling sites. **C:** ultra-high seismic profile of the Pompeia Escarpment, westwards of the Northern
 791 Pompeia Coral Ridge.
 792 seismic profile of the Pompeia Escarpment, westwards of the Northern Pompeia Ridge-



793 **Figure 3. Ultra-high resolution (A) and multichannel (B) seismic profiles showing geological features in southern**
 794 **Pompeia Province. Note mud diapirism has been described in this area (Vandorpe et al., 2017). OP = overpressure**
 795 **zone**
 796 **Seismic profiles showing geological features in the southern Pompeia Province. Note mud diapirism has been**
 797 **described in this area (Vandorpe et al., 2017). OP = overpressure zone.**



798

799

800

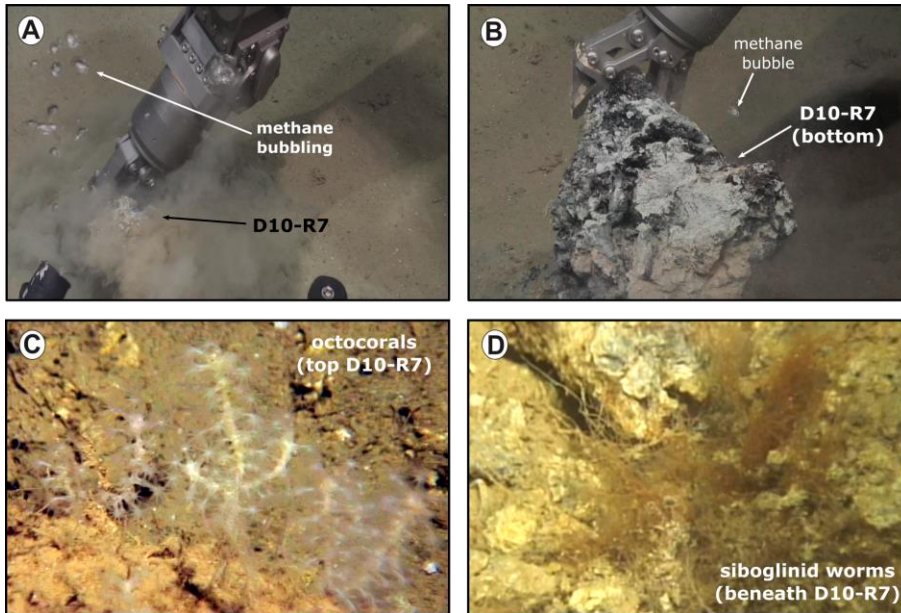
801

802

803

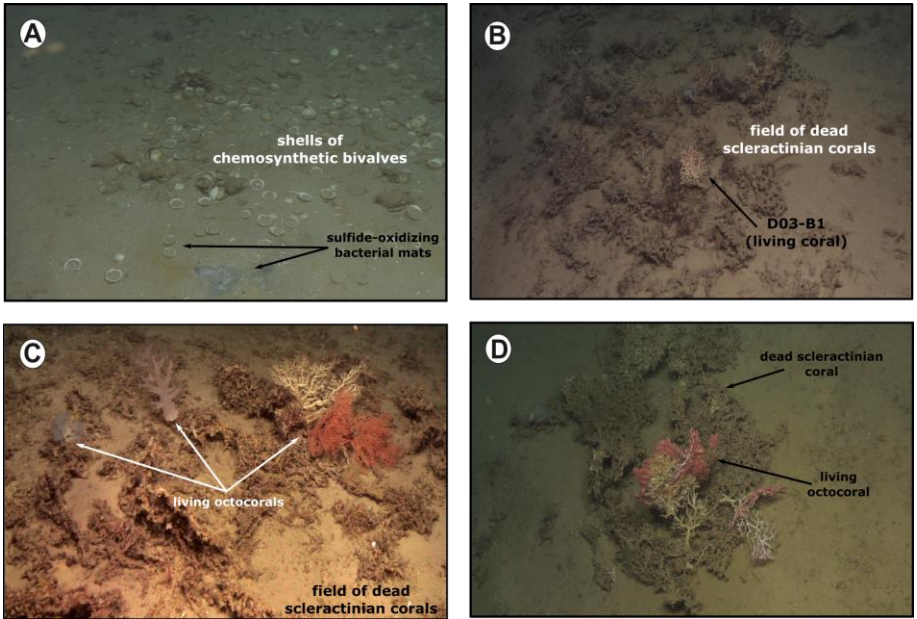
Figure 4: ROV still frames from the Al Gacel MV (Dives 10 and 11). **A:** eastern side of the volcano, displaying a field of sponges, corals and carbonates; **B–C:** active pockmark sites on the east side of the volcano, displaying authigenic carbonate surrounded by shells of chemosynthetic bivalves, fragments of scleractinian and octocorals, as well as sulfide-oxidizing bacterial mats; **D:** pockmark sites on the east side of the volcano, displaying authigenic

804 carbonate surrounded by shells of chemosynthetic bivalves, fragments of scleractinian and octocorals, as well as
805 sulfide oxidizing bacterial mats; D: metric-sized carbonate blocks located in a slope at the summit of the volcano.
806
807

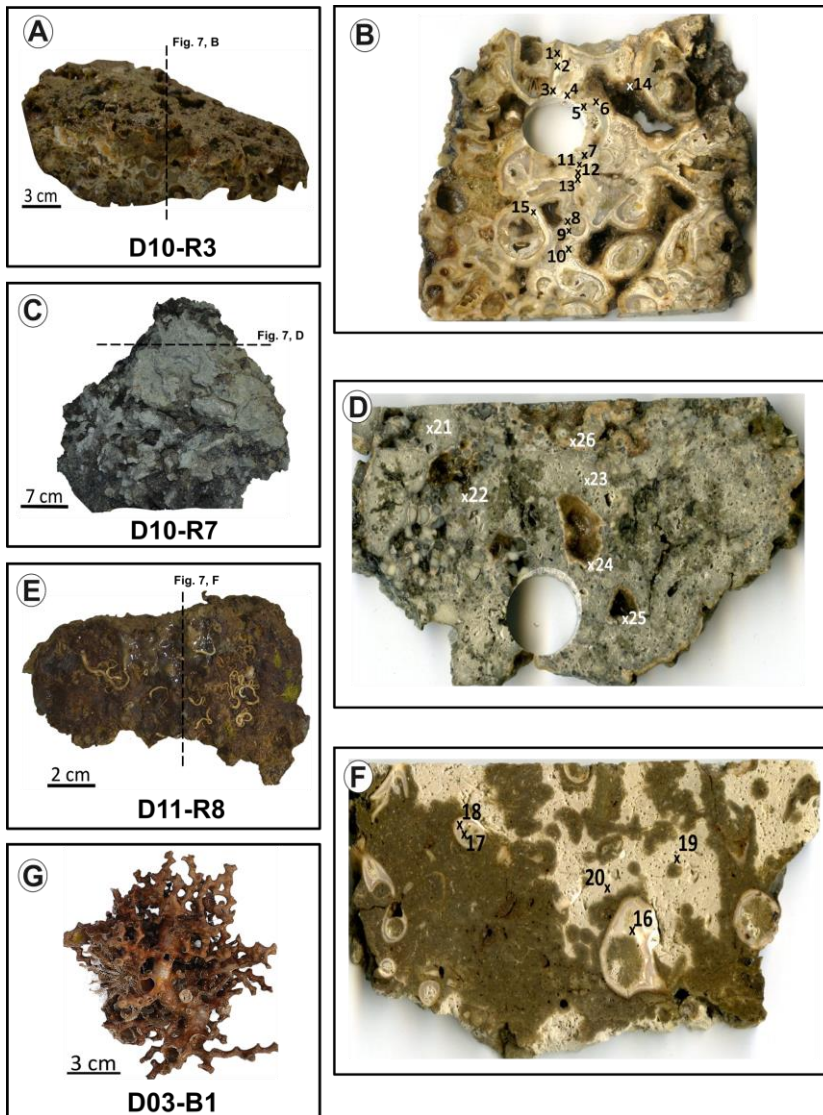


808
809 **Figure 5:** ROV still frames from the active pockmark site shown in Fig. 4. **A–B:** release of bubbles while
810 sampling; **C:** detailed photograph of the octocorals on top of the carbonate; **D:** detailed still frame from siboglinid
811 worms beneath the carbonate.

812
813
814

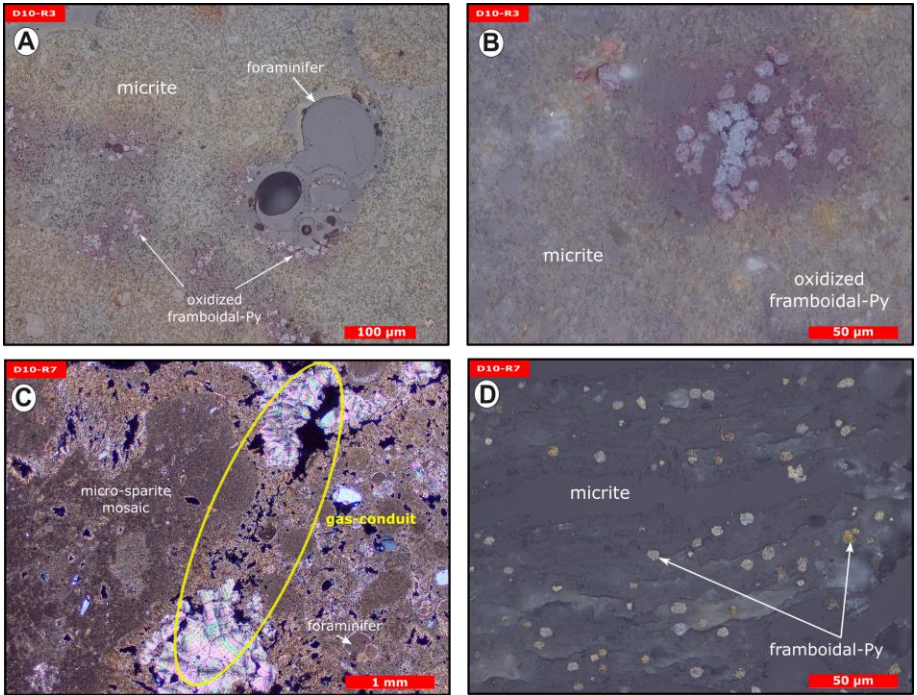


815
 816 **Figure 6.** ROV still frames from the Northern Pompeia Coral Ridge and extinct MV (Dive 03), where there is
 817 currently a diffused seepage of fluids. **A:** abundant shells of chemosynthetic bivalves with sulfide-oxidizing
 818 bacterial mats at the western site of the Northern Pompeia Coral Ridge; **B–D:** field of dead scleractinian-corals
 819 colonized by living corals; **D:** still frame from the extinct MV.
 820

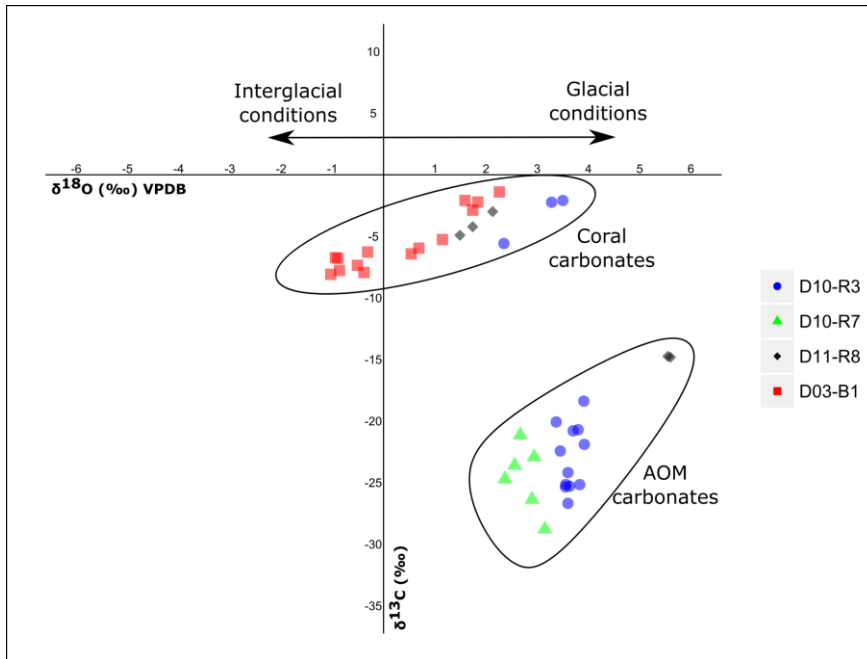


821
 822 **Figure 7.** Photographs of analyzed samples including sampling sites for stable carbon and oxygen isotope ($\delta^{13}\text{C}$,
 823 $\delta^{18}\text{O}$) analysis (crosses with numbers). Values of the stable isotopic analyses are found in Table 2. **A–B:** D10-R3
 824 carbonate with embedded corals; **C–D:** D10-R7 carbonate with strong H_2S odor; **E–F:** D11-R8 carbonate with
 825 embedded corals; **G:** D03-B1 scleractinian-coral fragment, *Madrepora oculata*.

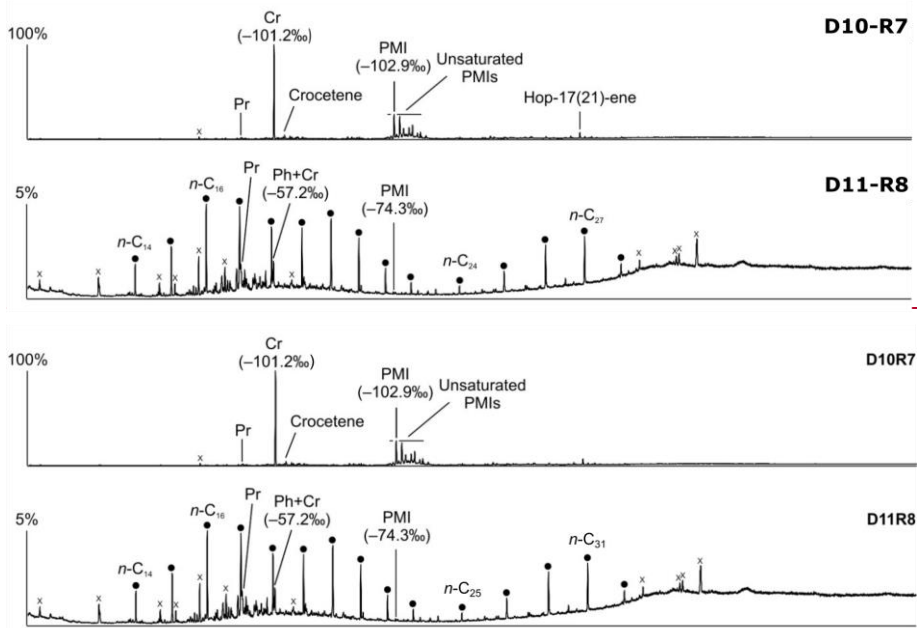
826
 827
 828



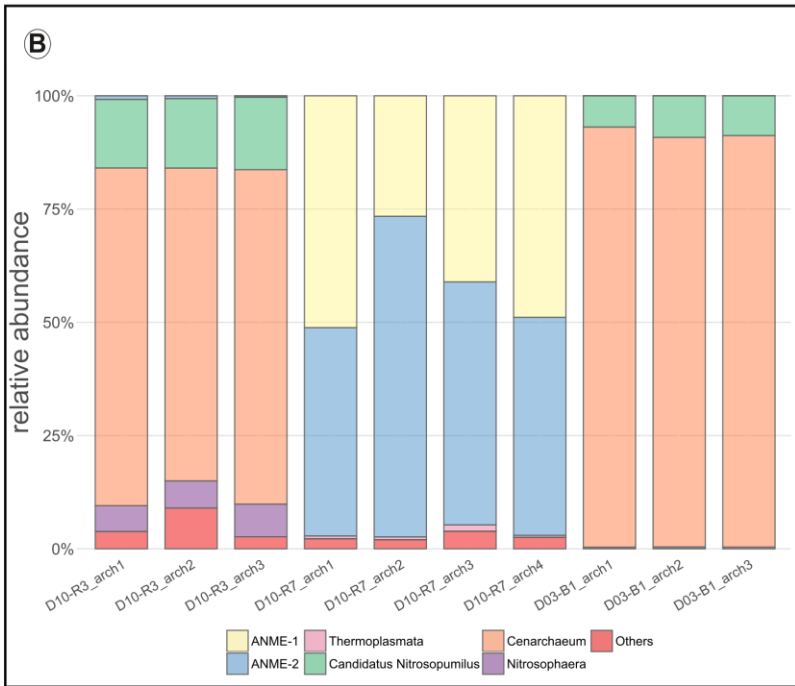
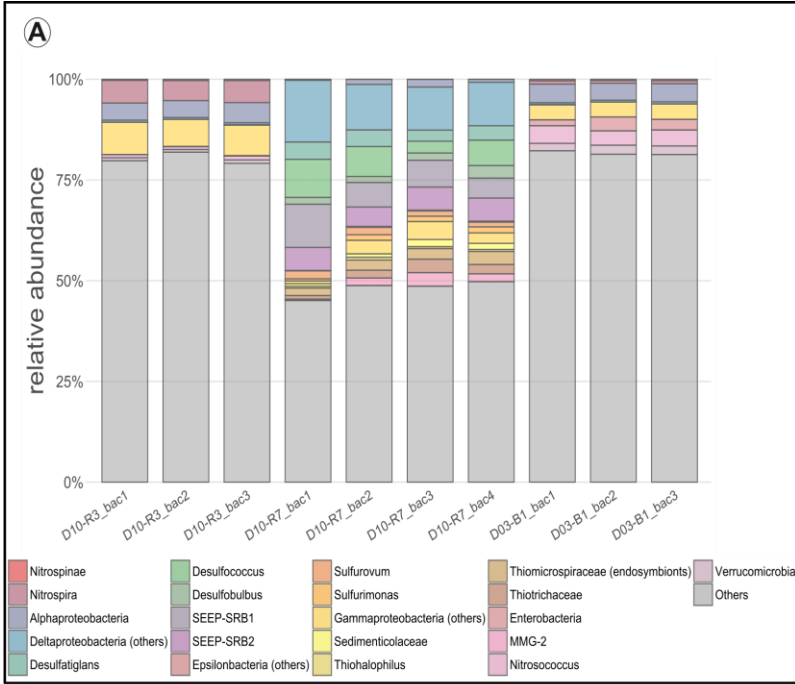
829
 830 **Figure 8.** Thin section photographs of MDACs. **A–B:** D10-R3 consisting of a micritic matrix with scattered
 831 foraminifers and oxidized framboidal pyrites (reflected light); **C–D:** D10-R7 consisting of micritic and micro-
 832 sparitic carbonate with abundant unaltered framboidal pyrites (C, transmitted light; D, reflected light). Please note
 833 open voids which represent potential pathways for fluid seepage (yellow circle in C).
 834

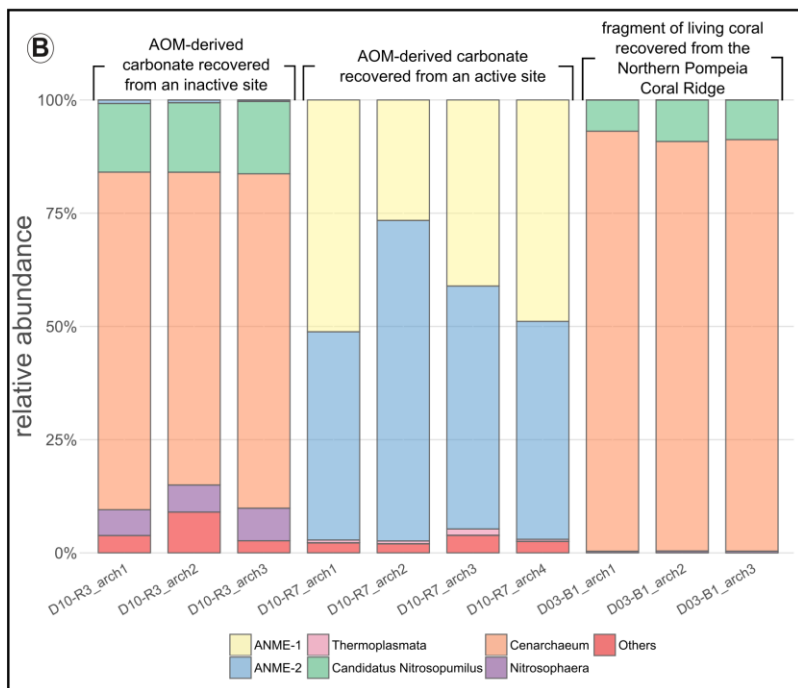
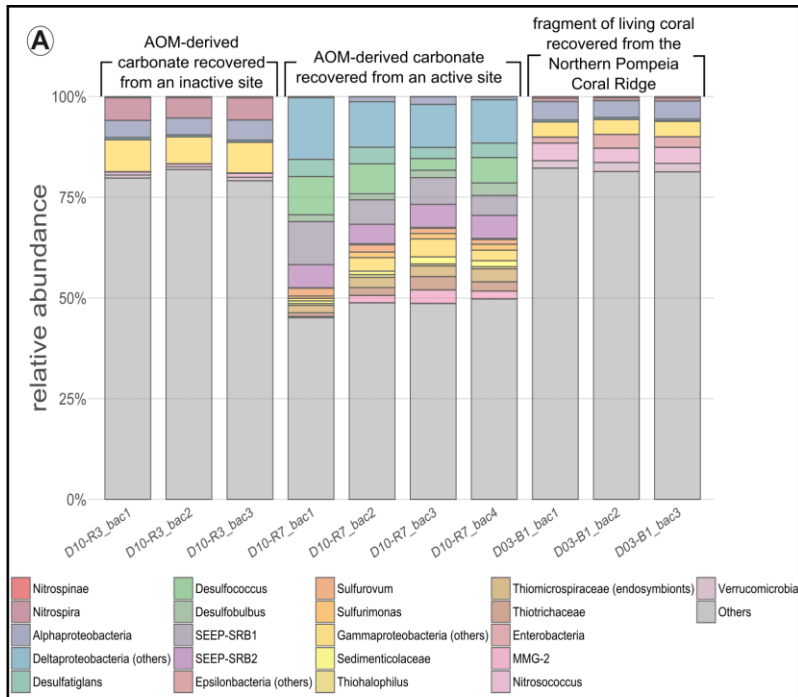


835
 836 **Figure 9.** Stable carbon and oxygen isotopes ($\delta^{13}\text{C}$, $\delta^{18}\text{O}$) of samples from the Al Gacel MV and the Northern
 837 Pompeia Coral Ridge (see **Figure 3** for precise sampling points).
 838
 839
 840
 841



842
843
844 **Figure 10.** Total ion current (TIC) chromatograms of the analyzed samples. Isotopically depleted acyclic irregular
845 isoprenoids such as Cr and PMI are typically found in settings influenced by the anaerobic oxidation of methane
846 (AOM). Pr = pristane; Ph = phytane; Cr = crocetane; PMI = 2,6,10,15,19-pentamethylcosane; dots = n-alkanes;
847 crosses = siloxanes (septum or column bleeding). Percentage values given on the vertical axes of chromatograms
848 relate peak intensities to highest peak (Cr in D10-R7).
849





852 **Figure 11.** Bar chart representing ~~relative abundances of prokaryotic taxa detected in each sample~~ ~~the different~~
853 ~~taxa found in each sample according to relative abundances.~~ **A:** bacterial taxa; **B:** archaeal taxa. In
854 “others” aggrupation is included taxa related to ubiquitous organism normally found in sea- and seepage-
855 related environments, and unclassified organisms. Number of reads per taxa detailed in **Table S1**
856 (bacteria) and **Table S2** (archaea).

Con formato: Sangría: Izquierda: 0 cm, Sangría francesa: 1,25 cm

Con formato: Fuente: Negrita

Con formato: Fuente: Negrita

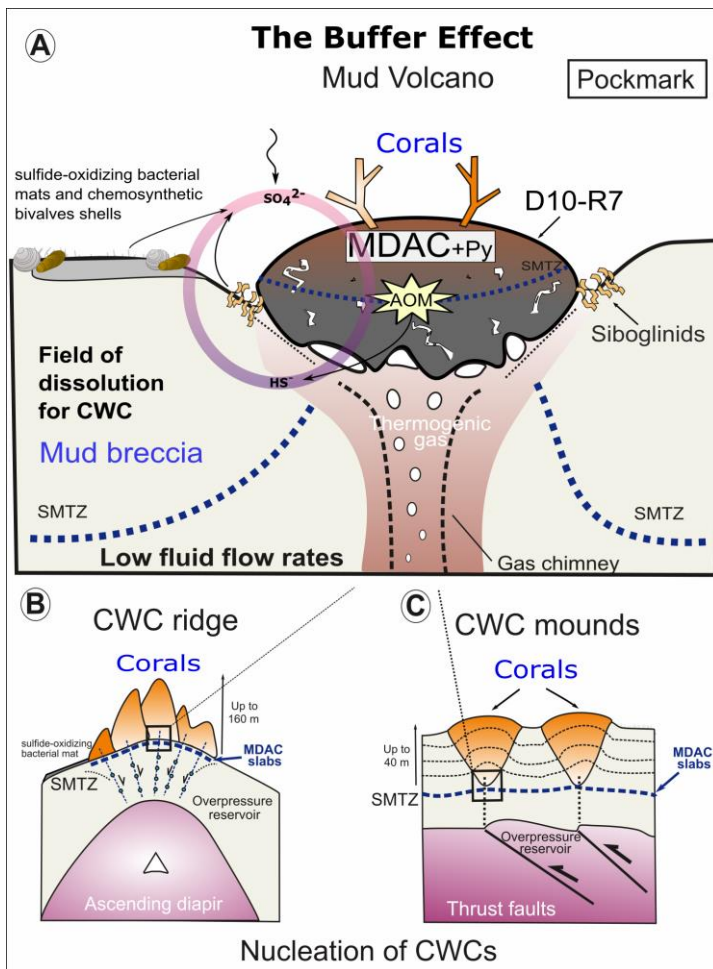


Figure 12. The buffer effect model. **A:** Buffer effect at pockmark sites (e.g. sampling site of D10-R7) where carbonates are formed directly on the bubbling site acting as a cap; **B:** Buffer effect at diapiric ridges where MDAC slabs are formed on the base of the ridge; **C:** Buffer effect at coral mounds where MDAC slabs are formed in deeper layers of the sediment. Py = pyrite, SMTZ: sulfur-methane transition zone.

860